
A Closer Look on Memorization in Tabular Diffusion Model: A Data-Centric Perspective

Zhengyu Fang¹, Zhimeng Jiang², Huiyuan Chen¹, Xiaoge Zhang¹, Kaiyu Tang¹,
Xiao Li^{1,3,4,5}, Jing Li¹

¹Department of Computer and Data Sciences, Case Western Reserve University

²Department of Computer Science & Engineering, Texas A&M University

³Department of Biochemistry, Case Western Reserve University

⁴Center for RNA Science and Therapeutics, Case Western Reserve University

⁵Department of Biomedical Engineering, Case Western Reserve University

zxf177@case.edu, zhimengj@tam.u.edu, hxc501@case.edu, xxz705@case.edu,
kxt439@case.edu, xx11015@case.edu, jingli@cwru.edu

Abstract

Diffusion models have shown strong performance in generating high-quality tabular data, but they carry privacy risks by inadvertently reproducing exact training samples. While prior work focuses on dataset-level augmentation for memorization mitigation, little is known about which individual samples contribute most to memorization. In this paper, we present the first *data-centric* study of *memorization dynamics* in tabular diffusion models. We begin by quantifying memorization for each real sample based on how many generated samples are flagged as its memorized replicas, using a relative distance ratio metric.¹ Our empirical analysis reveals a *heavy-tailed* distribution of memorization counts: a small subset of samples disproportionately contributes to leakage, a finding further validated through sample-removal experiments. To better understand this effect, we divide real samples into the top- and non-top-memorized groups (tags) and analyze their training-time behavior differences. We track *when* each sample is first memorized and monitor per-epoch *memorization intensity* (AUC) across groups. We find that memorized samples tend to be memorized slightly earlier and show significantly stronger memorization signals in early training stages. Based on these insights, we propose *DynamicCut*, a two-stage, model-agnostic mitigation method. *DynamicCut* (a) ranks real samples by their epoch-wise memorization intensity, (b) prunes a tunable top fraction, and (c) retrains the model on the filtered dataset. Across multiple benchmark tabular datasets and tabular diffusion models, *DynamicCut* reduces memorization ratios with negligible impact on data diversity and downstream task performance, and complements existing data augmentation methods for further memorization mitigation. Furthermore, *DynamicCut* has transferability across different generative models for memorization sample tagging, i.e., high-ranked samples identified from one model (e.g., a diffusion model) are also effective in reducing memorization when removed from other generative models such as GANs and VAEs.

¹We follow Yoon et al. [2023], Gu et al. [2023], Fang et al. [2024] to define sample memorization using the relative distance ratio.

1 Introduction

Tabular data generation has gained increasing attention due to its broad applicability in healthcare, finance, and digital platforms, supporting tasks such as data augmentation, privacy preservation, and counterfactual analysis Hernandez et al. [2022], Fonseca and Bacao [2023], Assefa et al. [2020]. Recent advances in generative modeling—particularly diffusion models have significantly improved the fidelity and diversity of synthetic tabular data Kotelnikov et al. [2023], Zhang et al. [2023], Yang et al. [2024], Shi et al. [2025]. These models outperform traditional GAN- or VAE-based approaches Xu et al. [2019] by offering better distributional coverage and sample quality across mixed-type and high-dimensional tabular domains. Despite the impressive performance of diffusion models in synthesizing high-quality tabular data, memorization remains a critical concern. In particular, tabular generative models risk reproducing individual training records that, while appearing structurally altered, still retain sensitive attributes of real individuals. This subtle form of privacy leakage violates core principles of generative modeling and has severe implications in sensitive domains such as healthcare and finance Karras et al. [2022], Carlini et al. [2021], Song et al. [2021], Ho et al. [2020]. To address this, prior work has primarily focused on memorization detection based on nearest-neighbor distance ratios and dataset-level augmentation strategies such as feature mixing TabCutMix Fang et al. [2024]. However, these methods fall short in two key ways. First, the memorization detection tool does not explain *when* or *which samples* are memorized during training. Second, the memorization mitigation method like TabCutMix operates uniformly across the dataset, ignoring the heterogeneous nature of sample-level memorization risks. This gap in understanding motivates a central question:

Can we proactively identify and mitigate memorization in tabular diffusion models by monitoring sample-level training dynamics in real time?

To answer this, we take a data-centric perspective and conduct the first fine-grained analysis of memorization dynamics in tabular diffusion models. Specifically, we seek to characterize: (1) **When** memorization arises during training; (2) **Which** samples are more likely to be memorized; (3) **How** memorization evolves and varies across examples. We show that memorization is not evenly distributed across samples: a small subset of training samples is disproportionately memorized. By tracking when each real sample is first memorized and quantifying its memorization intensity over epochs, we reveal strong early-stage signals that can be exploited to mitigate memorization.

Building on these insights, we propose a model-agnostic method for memorization mitigation, named **DynamicCut**, to identify and remove the samples with high-contribution memorization based on their early memorization intensity. DynamicCut can also be integrated into the existing data augmentation method TabCutMix, named **DynamicCutMix**, to further reduce memorization for tabular generative models. Our approach consistently reduces memorization across diverse datasets and generative models (e.g., TabDDPM, CTGAN, TVAE) without compromising data quality. Notably, the memorization mitigation benefits from samples with high-contribution memorization removal learned from one generative model can *generalize* to other generative models, demonstrating strong transferability and practicality.

2 Related Work

Tabular Generative Models. The generation of synthetic tabular data has attracted increasing attention with wide applications. Early methods such as TableGAN Park et al. [2018], CTGAN, and TVAE Xu et al. [2019] used GANs Goodfellow et al. [2020] and VAEs Kingma [2013] to address feature imbalance. Extensions like GANBLR Zhang et al. [2021] and VAE-BGM Apellániz et al. [2024] incorporate Bayesian structures to better model feature interactions and latent distributions.

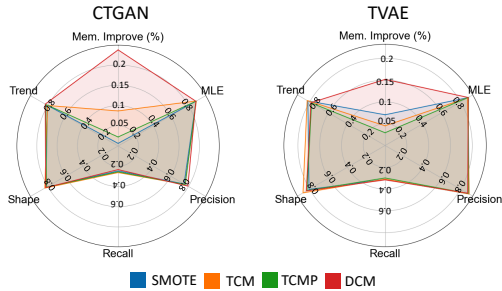


Figure 1: Overview of DynamicCutMix (DynamicCut + CutMix) performance in CTGAN and TVAE on Adult dataset. “Mem. Improve” denotes the normalized reduction in memorization ratio. Higher values, better mitigation effectiveness.

To enhance dependency modeling, GOGGLE Liu et al. [2023] uses graph neural networks, while GReaT Borisov et al. [2023] reformulates tabular rows as text for table-level modeling. Other alternatives include TabPFGen Ma et al. [2024], which employs a label-weighted Energy-Based Model with in-context learning. Recently, diffusion models—originally used in image generation Ho et al. [2020]—have shown strong performance on tabular data. Notable examples include STaSy Kim et al. [2023], TabDDPM Kotelnikov et al. [2023], CoDi Lee et al. [2023], TabSyn Zhang et al. [2023], Balanced Tabular Diffusion Yang et al. [2024], and TabDiff Shi et al. [2025].

Memorization in Generative Models. Memorization has been widely studied in image and language generation van den Burg and Williams [2021], Gu et al. [2023], Somepalli et al. [2023b], Wen et al. [2024], Hintersdorf et al. [2024], Huang et al. [2024], Shah et al. [2025], where models often replicate training data. In vision, diffusion models like Stable Diffusion Rombach et al. [2022] and DDPM Ho et al. [2020] exhibit memorization Somepalli et al. [2023a], Carlini et al. [2021], mitigated by methods such as concept ablation Kumari et al. [2023] and adaptive sample suppression Chen et al. [2024]. In language models, techniques like Goldfish Loss Hans et al. [2024] and early memorization prediction Biderman et al. [2024] aim to reduce overfitting to specific sequences. However, memorization in *tabular* data generation remains underexplored. Due to the structured and mixed-type nature of tabular data, understanding how memorization arises—and how it can be mitigated—presents a distinct and open research challenge.

3 Preliminary

3.1 Long-Tailed Distribution of Memorization Count

To understand the memorization behavior of diffusion-based tabular models, we conducted an empirical analysis using TabDDPM Kotelnikov et al. [2023] as a representative example. For each real training sample, we quantified sample-level memorization by counting the number of generated samples flagged as its replicas, based on the relative distance ratio criterion.

Obs.1: As shown in Figure 2, the distribution of memorization frequency exhibits a pronounced long-tail pattern. While most training samples are rarely memorized, a small subset is memorized far more frequently. This indicates an imbalance in how diffusion models recall training data during generation.

Obs.2: The existence of these high-frequency memorized samples suggest that certain instances disproportionately contribute to overall memorization. Understanding and characterizing these influential samples is crucial for uncovering the roots of memorization bias and assessing their implications for generation quality and privacy risk.

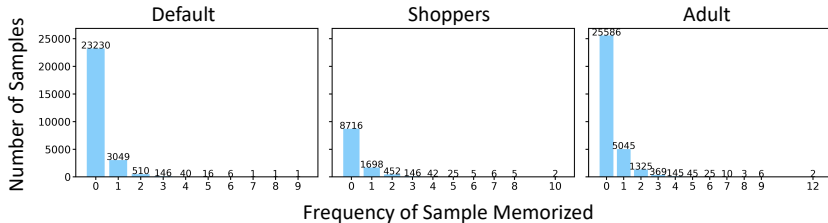


Figure 2: Memorization frequency per training sample shows a long-tail distribution, where a small number of samples are memorized much more frequently than others.

3.2 Tagging High-Memorization Samples

Building on the observed long-tailed distribution of sample-level memorization, we assign binary tags to training samples based on how frequently they are memorized during generation. Specifically, we rank all samples by their memorization count and define three threshold levels: the top 5%, top 10%, and top 20% most-memorized samples. Each sample is then tagged to indicate whether it falls within these high-risk subsets. These tags serve as the basis for analyzing memorization dynamics and designing targeted interventions.

3.3 Effectiveness of Targeted Sample Removal

To assess the practical impact of these high-memorization samples, we compare two intervention strategies: (1) randomly removing a specified portion of the training data, and (2) selectively removing the most-memorized samples as determined by our tagging. Table 1 presents memorization ratios for both strategies on the ADULT dataset.

Table 1: Comparison of memorization ratio after removing different subsets of training samples on the Adult dataset.

| Dataset | Method | Mem. Ratio (%) ↓ | Improv. |
|---------|-------------|------------------|----------|
| Adult | TabDDPM | 31.33 | – |
| | -Random 5% | 31.82 | –1.56% ↓ |
| | -Label 5% | 26.12 | 16.63% ↓ |
| | -Random 10% | 26.35 | 15.90% ↓ |
| | -Label 10% | 19.35 | 38.24% ↓ |
| | -Random 20% | 27.63 | 11.81% ↓ |
| | -Label 20% | 19.86 | 36.61% ↓ |

Obs.1: Selectively removing high-memorization samples consistently leads to greater reductions in memorization compared to random removal. For example, removing 10% of samples at random yields a 15.90% reduction in memorization, whereas removing the top 10% most-memorized samples achieves a 38.24% reduction. This trend holds across all tested removal levels (5%, 10%, 20%).

Obs.2: These results indicate that memorization is highly concentrated in a small subset of the training data. Consequently, even modest, targeted interventions can significantly mitigate

memorization without requiring extensive data removal, highlighting the potential for more efficient, privacy-preserving training strategies. Additional experimental results for tag performance are provided in Appendix A.5.

4 Closer Look at Memorization Dynamics During Training

Having identified high-memorization samples, we now investigate how memorization evolves throughout training. Specifically, we aim to understand *when* samples are memorized, *how* memorization persists or vanishes over time, and *what* dynamic patterns differentiate high-risk samples from others. This section formalizes memorization-related events and defines metrics to quantify memorization intensity.

4.1 Memorization and Forgetting: Event Definitions

We adopt the widely used relative distance ratio criterion Yoon et al. [2023], Gu et al. [2023], Fang et al. [2024] to determine whether a generated sample \mathbf{x} memorizes a real training sample. Formally, let \mathcal{D} be the training dataset and $d(\cdot, \cdot)$ be a distance metric in the input space. Let $\text{NN}_1(\mathbf{x})$ and $\text{NN}_2(\mathbf{x})$ denote the nearest and second-nearest training samples to \mathbf{x} , respectively. We define the distance ratio $r(\mathbf{x})$ as $r(\mathbf{x}) = \frac{d(\mathbf{x}, \text{NN}_1(\mathbf{x}, \mathcal{D}))}{d(\mathbf{x}, \text{NN}_2(\mathbf{x}, \mathcal{D}))}$. A sample \mathbf{x} is considered memorized if $r(\mathbf{x}) < \tau$,

where τ is a fixed memorization threshold (we follow prior work and use $\tau = \frac{1}{3}$).

Based on this definition, we track training-time dynamics at the level of individual real samples $\mathbf{x}_r \in \mathcal{D}$ by monitoring whether generated samples \mathbf{x}_g are repeatedly flagged as memorizing \mathbf{x}_r . We define the following events: **First Memorization:** The earliest training epoch when any generated sample satisfies $r(\mathbf{x}_g) < \tau$ for a given \mathbf{x}_r . **Forget Event:** A transition where \mathbf{x}_r was previously memorized but no longer satisfies the memorization criterion in subsequent epochs. **Cumulative Memorization Count:** The total number of times a sample is memorized during training. **Cumulative Forget Count:** The total number of transitions from memorization to non-memorization status.

To quantify the overall strength of memorization or forgetting, we adopt the *Memorization Area Under Curve* (Mem-AUC) Fang et al. [2024]. For each real sample \mathbf{x}_r , we track its minimum distance ratios $r(\mathbf{x}_g)$ across generated samples over training epochs and define: $\text{Mem-AUC}(\mathbf{x}_r) = \int_0^1 \mathbb{P}[r(\mathbf{x}_g) < \tau \mid \text{NN}_1(\mathbf{x}_g) = \mathbf{x}_r] d\tau$, where $\mathbb{P}[r(\mathbf{x}_g) < \tau]$ is the fraction of generated samples at each epoch that satisfy the memorization threshold τ for \mathbf{x}_r . Intuitively, higher Mem-AUC values indicate stronger and more persistent memorization behavior over time.

These event-based definitions and metrics form the basis of our dynamic analysis, where we compare high- and low-memorization samples for memorization dynamic analysis during training.

4.2 Temporal Dynamics of Memorization

Building on our tagging of high-memorization samples, we now investigate the temporal behavior of memorization throughout training. Figure 3 shows the cumulative proportion of samples memorized over training epochs, comparing the Top 5% most-memorized samples to the remaining Non-Top samples across three datasets.

Obs.1: Across all datasets—DEFAULT, SHOPPERS, and ADULT—the Top 5% samples are consistently memorized earlier (but not too much) than the Non-Top group. This persistent temporal gap suggests that high-memorization samples tend to enter the memorized state at earlier training stages.

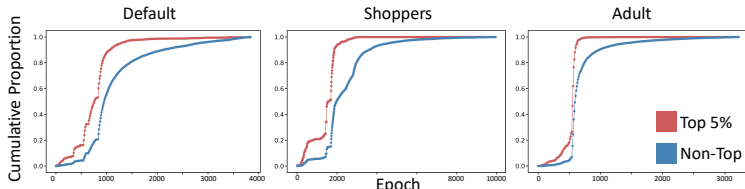


Figure 3: Cumulative proportion of samples memorized over epochs for Top 5% and Non-Top groups.

Obs.2: This early memorization behavior implies that Top samples may lie in regions of the data distribution that are more prominent or easier for the model to fit. These structural properties likely make them more susceptible to slightly early overfitting. Similar trends are observed for Top 10% and 20%, as shown in Appendix A.1.2.

4.3 Temporal Dynamics of Forgetting

Figure 4 (A) illustrates the distribution of forget events over time, comparing Top 5% and Non-Top samples.

Obs.1: Forget events for Top samples tend to occur earlier in training compared to Non-Top samples. This mirrors the earlier memorization trend observed in Figure 3, suggesting that samples memorized earlier also begin to be forgotten earlier. The alignment between early memorization and early forgetting indicates that Top samples are involved in learning dynamics from the beginning of training.

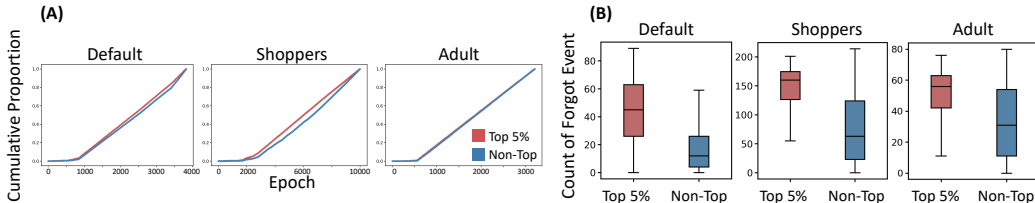


Figure 4: (A) Temporal dynamics of forget events for Top 5% and Non-Top samples. (B) Total number of forget events observed during training for Top 5% and Non-Top.

Obs.2: Figure 4 (B) further shows that the Top 5% samples accumulate a significantly higher number of forget events over training. This suggests that these samples are more volatile, frequently transitioning between memorized and non-memorized states. Such instability reflects a higher sensitivity to parameter updates and less stable retention, despite their prominent role in memorization. These patterns are consistent across all three datasets. Similar trends for the Top 10% and Top 20% groups are included in Appendix A.1.3.

4.4 Temporal Dynamics in Memorization Intensity

To quantify how memorization strength changes during training, we track the average Mem-AUC (memorization area under curve) over epochs for Top and Non-Top groups. Mem-AUC provides a smooth measure of memorization intensity over varying thresholds.

Obs.1: As shown in Figure 5, the Top 10% samples exhibit a sharp spike (**massive memorization intensity in a few epochs**) in Mem-AUC during early training, significantly higher than the Non-Top samples, whose memorization intensity grows gradually and remains low.

Obs.2: This early-stage peak suggests that memorization-prone samples can be identified early in training, without requiring full training-time monitoring. This opens up opportunities for early interventions, such as pruning, targeted regularization, or curriculum adjustments, to proactively reduce memorization risk and improve generalization.

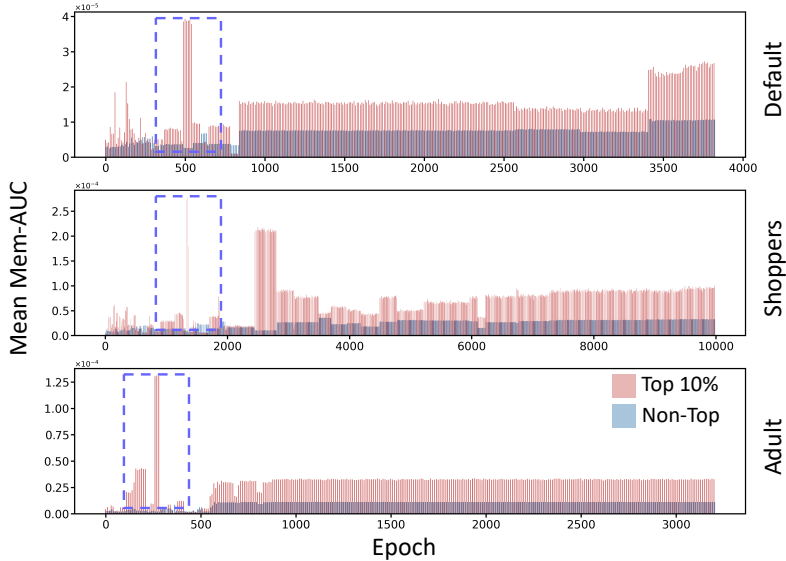


Figure 5: Mean Mem-AUC over training epochs for Top 10% and Non-Top samples. The sharp spike (massive memorization intensity in a few epochs) is illustrated in the blue box.

5 Methodology

5.1 Motivation

Our approach is driven by a series of consistent empirical findings observed in tabular diffusion models. First, memorization follows a pronounced long-tail distribution (Figure 2), with a small subset of training samples being memorized disproportionately often. These high-risk samples tend to be memorized early in training (Figure 3), exhibit volatile learning behavior with frequent forget-and-relearn cycles (Figure 4A), and contribute significantly to overall memorization. Selective removal of these samples reduces memorization much more effectively than random removal at the same rate (Table 1). Moreover, memorization intensity—measured via Mem-AUC—peaks in the early training stages (Figure 5), indicating that high-risk samples can be identified from only partial training trajectories. Together, these observations suggest that memorization is both *predictable* and *concentrated*, enabling targeted early-stage interventions to mitigate privacy risk while preserving data utility.

5.2 Algorithms

To operationalize these insights, we propose DynamicCut, a lightweight, model-agnostic filtering method that proactively identifies and removes memorization-prone samples based on early training dynamics (sharp peak memorization for high-risk samples).

Based on the observation that memorization-prone samples show strong signals early in training, we propose a lightweight filtering strategy that uses early Mem-AUC dynamics. For each training sample $\mathbf{x}_i \in \mathcal{D} = \{\mathbf{x}_1, \dots, \mathbf{x}_N\}$, we collect Mem-AUC values $\mathcal{A}_i = \{a_1(\mathbf{x}_i), \dots, a_T(\mathbf{x}_i)\}$ during the first T epochs. We then compute a memorization score s_i as the mean of the top- k highest values in \mathcal{A}_i , where $k = \lceil 0.1 \cdot T \rceil$. After ranking all samples by s_i , we remove the top p ratio with the highest scores, resulting in the filtered set $\mathcal{D}_{\text{filtered}} = \{\mathbf{x}_i \in \mathcal{D} \mid s_i < \tau\}$, where τ is the $(1 - p)$ quantile. We use $p = 0.1$ by default.

Table 2: The overview performance comparison for DynamicCut methods on different datasets. “DC” represents our proposed **DynamicCut**. “Mem. Ratio” represents memorization ratio. “Improv” represents the improvement ratio on memorization.

| | Methods | Mem. Ratio (%) ↓ | Improv. | MLE (%) ↑ | α -Precision (%) ↑ | β -Recall (%) ↑ | Shape Score (%) ↑ | Trend Score (%) ↑ | C2ST (%) ↑ | DCR (%) |
|----------|------------|------------------|-----------------|--------------|---------------------------|-----------------------|-------------------|-------------------|--------------|--------------|
| Default | TabDDPM | 19.33 ± 0.45 | - | 76.79 ± 0.69 | 98.15 ± 1.45 | 44.41 ± 0.70 | 97.58 ± 0.95 | 94.46 ± 0.68 | 91.85 ± 6.04 | 49.12 ± 0.94 |
| | TabDDPM+DC | 18.69 ± 1.04 | 3.31% ↓ | 76.42 ± 0.73 | 93.26 ± 5.44 | 42.64 ± 1.16 | 93.40 ± 3.46 | 89.65 ± 4.00 | 86.09 ± 6.48 | 50.78 ± 1.60 |
| | CTGAN | 12.83 ± 0.63 | - | 68.68 ± 0.21 | 68.95 ± 1.70 | 16.49 ± 0.55 | 85.04 ± 0.93 | 77.05 ± 2.47 | 61.89 ± 4.89 | 49.45 ± 0.80 |
| | CTGAN+DC | 12.60 ± 0.20 | 1.79% ↓ | 70.04 ± 0.66 | 69.06 ± 3.69 | 16.46 ± 0.97 | 85.11 ± 0.20 | 77.03 ± 0.41 | 58.03 ± 5.65 | 50.93 ± 1.82 |
| | TVAE | 17.22 ± 0.43 | - | 72.24 ± 0.36 | 82.97 ± 0.37 | 20.57 ± 0.42 | 89.37 ± 0.54 | 83.36 ± 0.99 | 52.63 ± 0.37 | 51.33 ± 0.96 |
| | TVAE+DC | 16.75 ± 0.60 | 2.73% ↓ | 76.87 ± 0.54 | 82.54 ± 1.97 | 21.25 ± 0.60 | 89.98 ± 0.74 | 80.36 ± 0.63 | 51.42 ± 3.67 | 50.01 ± 2.21 |
| Shoppers | TabDDPM | 31.37 ± 0.31 | - | 92.17 ± 0.32 | 93.16 ± 1.58 | 52.57 ± 1.30 | 97.08 ± 0.46 | 92.92 ± 3.27 | 86.74 ± 0.63 | 51.36 ± 0.63 |
| | TabDDPM+DC | 29.41 ± 2.38 | 6.66% ↓ | 91.08 ± 1.18 | 91.88 ± 2.74 | 52.74 ± 2.67 | 93.56 ± 2.89 | 89.40 ± 3.87 | 80.12 ± 4.54 | 51.87 ± 0.23 |
| | CTGAN | 19.80 ± 1.15 | - | 83.22 ± 1.30 | 85.26 ± 5.17 | 26.67 ± 1.66 | 77.73 ± 0.50 | 86.48 ± 0.69 | 67.18 ± 5.84 | 48.54 ± 0.74 |
| | CTGAN+DC | 19.64 ± 0.45 | 0.81% ↓ | 83.71 ± 0.44 | 89.13 ± 4.17 | 27.73 ± 0.66 | 77.78 ± 0.87 | 86.93 ± 0.34 | 69.31 ± 6.11 | 48.55 ± 1.50 |
| | TVAE | 23.17 ± 0.77 | - | 86.65 ± 0.48 | 50.32 ± 2.98 | 11.16 ± 1.33 | 74.75 ± 0.92 | 77.56 ± 1.11 | 21.29 ± 3.28 | 43.31 ± 0.65 |
| | TVAE+DC | 22.65 ± 0.83 | 2.24% ↓ | 86.93 ± 0.38 | 50.61 ± 1.39 | 12.49 ± 0.85 | 74.66 ± 0.73 | 79.14 ± 0.30 | 21.38 ± 2.28 | 47.61 ± 5.38 |
| Adult | TabDDPM | 31.01 ± 0.18 | - | 91.09 ± 0.07 | 93.58 ± 1.99 | 51.52 ± 2.29 | 98.84 ± 0.03 | 97.78 ± 0.07 | 94.63 ± 1.19 | 51.56 ± 0.34 |
| | TabDDPM+DC | 26.80 ± 1.03 | 13.58% ↓ | 90.81 ± 0.29 | 97.45 ± 1.20 | 45.54 ± 1.32 | 95.68 ± 2.55 | 93.62 ± 2.82 | 86.84 ± 3.48 | 50.42 ± 1.24 |
| | CTGAN | 21.68 ± 0.62 | - | 88.64 ± 0.32 | 78.15 ± 3.66 | 26.27 ± 0.67 | 82.43 ± 0.90 | 82.83 ± 0.93 | 63.64 ± 2.74 | 49.14 ± 0.27 |
| | CTGAN+DC | 16.64 ± 0.27 | 23.25% ↓ | 88.23 ± 0.67 | 74.41 ± 1.07 | 23.52 ± 0.92 | 81.08 ± 1.56 | 83.26 ± 1.00 | 61.72 ± 4.20 | 48.14 ± 0.51 |
| | TVAE | 30.78 ± 0.41 | - | 88.61 ± 0.49 | 92.34 ± 2.19 | 29.90 ± 1.00 | 82.71 ± 0.45 | 79.06 ± 0.90 | 48.67 ± 2.70 | 48.76 ± 0.25 |
| | TVAE+DC | 25.93 ± 1.10 | 15.76% ↓ | 88.25 ± 0.33 | 87.80 ± 0.74 | 30.57 ± 2.82 | 83.54 ± 0.56 | 78.71 ± 0.86 | 55.64 ± 2.59 | 45.96 ± 0.54 |

6 Experiments

In this section, we extensively evaluate the effectiveness of DynamicCut and DynamicCutMix across several SOTA tabular diffusion models in various datasets and compare other augmentation methods SMOTE Chawla et al. [2002], TabCutMix Fang et al. [2024] and TabCutMixPlus Fang et al. [2024].

6.1 Experimental Setup

Datasets. We utilize three real-world tabular datasets—Adult, Default, and Shoppers—each comprising both numerical and categorical features. Detailed descriptions and summary statistics for these datasets can be found in the Appendix C.4.

Models. We integrate DynamicCut into three generative models for tabular data: TabDDPM Kotelnikov et al. [2023], CTGAN Xu et al. [2019], and TVAE Xu et al. [2019]. This integration enables a comprehensive evaluation of each model’s generation quality and memorization behavior when enhanced with DynamicCut. More detailed information about these diffusion models can be found in the Appendix C.2

Evaluation Metrics. We evaluate the performance of synthetic data generation from two perspectives: memorization and synthetic data quality. For memorization evaluation, we generate the same number of synthetic samples as the training dataset and follow C.3 to calculate the distance between the generated and real samples. For synthetic data quality evaluation, we consider 1) low-order statistics (i.e., column-wise density and pair-wise column correlation) measured by shape score and trend score; 2) high-order metrics α -precision and β -recall scores measuring the overall fidelity and diversity of synthetic data; 3) downstream tasks performance machine learning efficiency (MLE); 4) C2ST (Classifier Two-Sample Test) evaluates data quality by measuring how well a classifier can distinguish real from synthetic data—lower accuracy suggests better distributional alignment; 5) DCR (Distance to Closest Record) measures privacy risk by quantifying how closely a synthetic sample resembles training vs. holdout samples—lower differences indicate better privacy preservation. The reported results are averaged over 5 independent experimental runs. More details on evaluation metrics can be found in Zhang et al. [2023], Fang et al. [2024].

6.2 Unified Evaluation of Memorization under Data Quality and Training Dynamics

Table 2 presents a comprehensive comparison of generative models with and without our proposed DC strategy across three datasets: DEFAULT, SHOPPERS, and ADULT.

Obs.1: Across all model–dataset combinations, the application of DC consistently reduces the memorization ratio. For instance, TabDDPM’s memorization ratio drops from 31.01% to 26.80% on the ADULT dataset, representing a 13.58% relative decrease. On DEFAULT and SHOPPERS, similar reductions are observed (e.g., 3.31% and 6.66% for TabDDPM, respectively). Notably, CTGAN and TVAE—two fundamentally different model families—also benefit from DC, with up to 23.25% and 15.76% memorization reduction on ADULT. These consistent gains confirm that DC is broadly effective across different model architectures and data regimes.

Obs.2: Importantly, the improvement in memorization does not come at the cost of substantial degradation in downstream utility. For example, although α -Precision and β -Recall occasionally exhibit small drops, metrics like Shape Score, Trend Score, and MLE remain stable or even improve in some cases. On DEFAULT, TabDDPM+DC maintains a high shape score (93.40%) and trend score (89.65%), only slightly lower than the baseline.

These results highlight that DynamicCut offers a principled and effective solution to control memorization risk without significantly sacrificing generation quality, making it a practical add-on for improving both the fidelity and safety of tabular generative models. Additional tag ratio and hyperparameter studies are provided in Appendix A.1 and A.3.

Table 3: The overview performance comparison for tabular models on different datasets. ‘‘DCM’’ represents our proposed **DynamicCutMix**.

| | Methods | Mem. Ratio (%) ↓ | Improv. | MLE (%) ↑ | α -Precision (%) ↑ | β -Recall (%) ↑ | Shape Score (%) ↑ | Trend Score (%) ↑ | C2ST (%) ↑ | DCR (%) |
|----------|---------------|------------------|-----------------|--------------|---------------------------|-----------------------|-------------------|-------------------|---------------|--------------|
| Default | TabDDPM | 19.33 ± 0.45 | - | 76.79 ± 0.69 | 98.15 ± 1.45 | 44.41 ± 0.70 | 97.58 ± 0.95 | 94.46 ± 0.68 | 91.85 ± 6.04 | 49.12 ± 0.94 |
| | TabDDPM+SMOTE | 17.46 ± 0.51 | 9.66% ↓ | 76.92 ± 0.35 | 91.19 ± 0.68 | 40.52 ± 0.65 | 94.89 ± 1.46 | 28.63 ± 2.28 | 72.73 ± 0.69 | 50.95 ± 0.38 |
| | TabDDPM+TCM | 16.76 ± 0.47 | 13.26% ↓ | 76.47 ± 0.60 | 97.30 ± 0.46 | 38.72 ± 2.78 | 97.27 ± 1.74 | 93.27 ± 2.52 | 94.72 ± 3.87 | 50.23 ± 0.53 |
| | TabDDPM+TCMP | 18.00 ± 0.24 | 6.88% ↓ | 76.92 ± 0.17 | 98.26 ± 0.25 | 41.92 ± 0.52 | 97.37 ± 0.09 | 91.42 ± 1.15 | 95.64 ± 0.49 | 49.75 ± 0.32 |
| | TabDDPM+DCM | 15.79 ± 2.06 | 18.31% ↓ | 76.68 ± 0.76 | 91.97 ± 1.78 | 37.89 ± 0.84 | 93.62 ± 2.78 | 89.30 ± 3.02 | 87.63 ± 2.15 | 48.17 ± 2.59 |
| | CTGAN | 12.83 ± 0.63 | - | 68.68 ± 0.21 | 68.95 ± 1.70 | 16.49 ± 0.55 | 85.04 ± 0.93 | 77.05 ± 2.47 | 61.89 ± 4.89 | 49.45 ± 0.80 |
| | CTGAN+SMOTE | 13.56 ± 0.41 | -5.69% ↓ | 71.23 ± 1.54 | 65.18 ± 2.81 | 17.13 ± 0.20 | 84.31 ± 0.20 | 31.76 ± 0.11 | 56.35 ± 0.60 | 49.05 ± 2.85 |
| | CTGAN+TCM | 12.87 ± 0.28 | -0.03% ↓ | 73.21 ± 0.45 | 75.30 ± 2.12 | 16.63 ± 0.27 | 85.77 ± 0.13 | 76.69 ± 1.20 | 58.62 ± 5.34 | 49.90 ± 3.12 |
| | CTGAN+TCMP | 11.80 ± 0.25 | 8.03% ↓ | 70.05 ± 0.81 | 71.33 ± 0.82 | 17.02 ± 0.60 | 85.28 ± 0.97 | 78.09 ± 0.32 | 63.67 ± 3.07 | 50.14 ± 0.60 |
| | CTGAN+DCM | 12.47 ± 0.07 | 2.81% ↓ | 72.37 ± 0.39 | 71.72 ± 0.74 | 16.64 ± 0.20 | 85.78 ± 0.70 | 76.85 ± 1.62 | 57.98 ± 3.09 | 48.48 ± 0.24 |
| | TVAE | 17.22 ± 0.43 | - | 72.24 ± 0.36 | 82.97 ± 0.37 | 20.57 ± 0.42 | 89.37 ± 0.54 | 83.36 ± 0.99 | 52.63 ± 0.37 | 51.33 ± 0.96 |
| | TVAE+SMOTE | 15.64 ± 0.41 | 9.18% ↓ | 75.41 ± 0.42 | 82.47 ± 0.42 | 20.77 ± 0.73 | 88.79 ± 0.08 | 79.34 ± 2.40 | 53.28 ± 3.26 | 49.20 ± 1.54 |
| | TVAE+TCM | 16.42 ± 0.37 | 4.65% ↓ | 75.05 ± 0.66 | 80.23 ± 2.07 | 21.90 ± 2.36 | 89.65 ± 0.15 | 80.15 ± 0.75 | 52.10 ± 4.29 | 49.99 ± 1.78 |
| | TVAE+TCMP | 15.59 ± 0.28 | 9.47% ↓ | 72.75 ± 0.52 | 81.57 ± 0.32 | 19.52 ± 0.39 | 89.33 ± 0.48 | 78.04 ± 6.05 | 45.60 ± 0.90 | 50.07 ± 0.52 |
| | TVAE+DCM | 16.32 ± 0.21 | 5.23% ↓ | 76.27 ± 0.25 | 85.49 ± 0.41 | 21.66 ± 0.19 | 90.36 ± 0.25 | 86.76 ± 5.13 | 54.81 ± 0.79 | 51.07 ± 1.35 |
| Shoppers | TabDDPM | 31.37 ± 0.31 | - | 92.17 ± 0.32 | 93.16 ± 1.58 | 52.57 ± 1.30 | 97.08 ± 0.46 | 92.92 ± 3.27 | 86.74 ± 0.63 | 51.36 ± 0.63 |
| | TabDDPM+SMOTE | 26.64 ± 1.46 | 15.07% ↓ | 89.96 ± 0.95 | 94.41 ± 4.67 | 45.22 ± 3.26 | 90.78 ± 0.49 | 83.09 ± 2.47 | 64.05 ± 1.44 | 51.94 ± 1.52 |
| | TabDDPM+TCM | 25.56 ± 1.17 | 18.51% ↓ | 92.17 ± 0.26 | 94.41 ± 1.49 | 50.05 ± 1.59 | 97.18 ± 0.34 | 93.95 ± 0.51 | 86.96 ± 0.50 | 47.52 ± 1.81 |
| | TabDDPM+TCMP | 28.51 ± 0.35 | 9.12% ↓ | 92.09 ± 0.99 | 93.43 ± 1.65 | 52.30 ± 0.73 | 97.31 ± 0.22 | 94.79 ± 0.30 | 87.02 ± 2.04 | 50.83 ± 0.59 |
| | TabDDPM+DCM | 24.24 ± 2.83 | 22.73% ↓ | 91.46 ± 0.74 | 93.25 ± 3.87 | 46.15 ± 4.42 | 92.32 ± 5.00 | 89.11 ± 4.95 | 80.56 ± 4.81 | 49.74 ± 3.34 |
| | CTGAN | 19.80 ± 1.15 | - | 83.22 ± 1.30 | 85.26 ± 5.17 | 26.67 ± 1.66 | 77.73 ± 0.50 | 86.48 ± 0.69 | 67.18 ± 5.84 | 48.54 ± 0.74 |
| | CTGAN+SMOTE | 20.53 ± 1.86 | -3.69% ↓ | 87.09 ± 1.22 | 76.13 ± 13.12 | 26.19 ± 3.66 | 75.57 ± 2.48 | 83.94 ± 1.13 | 59.83 ± 6.67 | 50.74 ± 1.75 |
| | CTGAN+TCM | 19.06 ± 0.42 | 3.74% ↓ | 84.21 ± 1.21 | 80.82 ± 7.68 | 26.50 ± 1.50 | 77.51 ± 2.15 | 85.75 ± 1.31 | 62.04 ± 6.75 | 49.90 ± 2.33 |
| | CTGAN+TCMP | 19.69 ± 0.35 | 0.52% ↓ | 83.94 ± 0.80 | 82.07 ± 9.62 | 23.47 ± 0.43 | 76.15 ± 0.22 | 84.56 ± 0.40 | 64.60 ± 0.82 | 52.02 ± 0.13 |
| | CTGAN+DCM | 18.71 ± 0.56 | 5.51% ↓ | 85.51 ± 0.46 | 83.51 ± 1.60 | 26.19 ± 0.82 | 78.23 ± 0.30 | 86.36 ± 0.47 | 68.85 ± 2.45 | 50.64 ± 1.11 |
| | TVAE | 23.17 ± 0.77 | - | 86.65 ± 0.48 | 50.32 ± 2.98 | 11.16 ± 1.33 | 74.75 ± 0.92 | 77.56 ± 1.11 | 21.29 ± 3.28 | 43.31 ± 0.65 |
| | TVAE+SMOTE | 19.77 ± 0.39 | 14.67% ↓ | 89.71 ± 0.69 | 52.39 ± 3.94 | 13.74 ± 0.54 | 71.80 ± 0.63 | 76.20 ± 0.68 | 20.67 ± 2.34 | 47.42 ± 3.40 |
| | TVAE+TCM | 20.81 ± 2.38 | 10.19% ↓ | 87.33 ± 0.90 | 49.75 ± 5.04 | 12.66 ± 3.18 | 75.47 ± 1.30 | 78.91 ± 1.30 | 21.87 ± 3.87 | 50.06 ± 1.78 |
| | TVAE+TCMP | 20.16 ± 0.80 | 12.98% ↓ | 87.07 ± 0.74 | 50.69 ± 0.44 | 10.54 ± 1.68 | 74.86 ± 0.26 | 78.55 ± 0.48 | 21.78 ± 4.28 | 43.21 ± 0.69 |
| | TVAE+DCM | 20.30 ± 1.33 | 12.39% ↓ | 88.32 ± 0.29 | 51.12 ± 2.46 | 11.98 ± 0.58 | 75.02 ± 0.97 | 79.02 ± 0.12 | 22.99 ± 2.12 | 49.98 ± 2.55 |
| Adult | TabDDPM | 31.01 ± 0.18 | - | 91.09 ± 0.07 | 93.58 ± 1.99 | 51.52 ± 2.29 | 98.84 ± 0.03 | 97.78 ± 0.07 | 94.63 ± 1.19 | 51.56 ± 0.34 |
| | TabDDPM+SMOTE | 28.98 ± 0.78 | 6.56% ↓ | 90.41 ± 0.36 | 94.93 ± 1.72 | 46.10 ± 0.65 | 93.40 ± 1.12 | 90.76 ± 1.76 | 80.75 ± 0.84 | 51.82 ± 0.56 |
| | TabDDPM+TCM | 27.55 ± 0.19 | 11.16% ↓ | 91.15 ± 0.06 | 94.97 ± 0.06 | 47.43 ± 1.46 | 98.65 ± 0.03 | 97.75 ± 0.07 | 85.61 ± 16.03 | 50.99 ± 0.65 |
| | TabDDPM+TCMP | 26.10 ± 2.11 | 15.83% ↓ | 90.54 ± 0.17 | 92.26 ± 6.97 | 43.49 ± 3.74 | 95.10 ± 4.27 | 91.50 ± 6.53 | 84.76 ± 10.12 | 50.68 ± 0.89 |
| | TabDDPM+DCM | 26.27 ± 0.57 | 15.29% ↓ | 90.81 ± 0.16 | 95.23 ± 1.14 | 45.76 ± 1.02 | 98.27 ± 0.32 | 96.71 ± 0.86 | 92.64 ± 1.65 | 50.79 ± 0.46 |
| | CTGAN | 21.68 ± 0.62 | - | 88.64 ± 0.32 | 78.15 ± 3.66 | 26.27 ± 0.67 | 82.43 ± 0.90 | 82.83 ± 0.93 | 63.64 ± 2.74 | 49.14 ± 0.27 |
| | CTGAN+SMOTE | 21.54 ± 0.69 | 0.65% ↓ | 88.59 ± 0.41 | 74.96 ± 5.01 | 24.65 ± 1.44 | 82.16 ± 1.14 | 80.23 ± 0.38 | 60.01 ± 2.10 | 51.71 ± 2.15 |
| | CTGAN+TCM | 19.80 ± 0.48 | 8.67% ↓ | 88.94 ± 0.64 | 76.10 ± 4.79 | 26.29 ± 1.53 | 83.26 ± 1.30 | 80.09 ± 1.89 | 61.16 ± 3.59 | 49.87 ± 0.64 |
| | CTGAN+TCMP | 21.20 ± 0.31 | 2.23% ↓ | 88.63 ± 0.66 | 76.27 ± 0.60 | 25.56 ± 0.33 | 81.42 ± 0.32 | 82.11 ± 1.01 | 60.98 ± 1.67 | 50.96 ± 0.17 |
| | CTGAN+DCM | 16.53 ± 0.88 | 23.75% ↓ | 88.45 ± 0.29 | 79.31 ± 1.04 | 23.31 ± 1.42 | 82.23 ± 0.23 | 82.80 ± 2.27 | 63.46 ± 3.43 | 48.13 ± 0.33 |
| | TVAE | 30.78 ± 0.41 | - | 88.61 ± 0.49 | 92.34 ± 2.19 | 29.90 ± 1.00 | 82.71 ± 0.45 | 79.06 ± 0.90 | 48.67 ± 2.70 | 48.76 ± 0.25 |
| | TVAE+SMOTE | 28.61 ± 0.16 | 7.05% ↓ | 87.89 ± 0.32 | 89.00 ± 3.48 | 31.01 ± 2.50 | 80.65 ± 1.28 | 81.83 ± 1.64 | 52.98 ± 6.01 | 50.37 ± 0.76 |
| | TVAE+TCM | 29.39 ± 0.58 | 4.52% ↓ | 87.33 ± 0.90 | 89.01 ± 5.77 | 30.87 ± 2.48 | 87.00 ± 2.13 | 82.57 ± 1.56 | 54.98 ± 7.02 | 49.43 ± 0.04 |
| | TVAE+TCMP | 29.88 ± 0.34 | 2.93% ↓ | 88.42 ± 0.26 | 88.02 ± 0.72 | 29.78 ± 1.42 | 82.76 ± 0.92 | 77.92 ± 0.66 | 52.52 ± 7.24 | 51.35 ± 0.29 |
| | TVAE+DCM | 26.11 ± 0.45 | 15.17% ↓ | 88.12 ± 0.32 | 87.54 ± 1.24 | 31.54 ± 0.38 | 83.45 ± 0.84 | 78.57 ± 0.68 | 54.85 ± 5.05 | 48.81 ± 2.10 |

6.3 DynamicCut with TabCutMix (DynamicCutMix): Combined Effect and Evaluation

Table 3 summarizes the performance of our proposed DCM method, which combines memorization-aware filtering (DC) with data augmentation (TCM). We evaluate DCM on three generative models (TabDDPM, CTGAN, TVAE) and three datasets (DEFAULT, SHOPPERS, ADULT), comparing it to strong baselines including TCM, TCMP, and SMOTE.

Obs.1: DCM consistently achieves the lowest memorization ratios. For example, on DEFAULT with TabDDPM, DCM reduces memorization to 15.79%, outperforming TCM (16.76%) and TCMP (18.00%). Similar patterns are observed across other models and datasets.

Obs.2: DCM also maintains strong utility. On ADULT, TabDDPM+DCM yields a Shape Score of 98.27% and a Trend Score of 96.71%, outperforming SMOTE and matching or exceeding TCM and TCMP. This demonstrates DCM’s ability to balance memorization reduction with sample quality.

Table 4: Comparison of memorization mitigation Transferability performance for tabular models under different tagging sources. “DCM” represents our proposed **DynamicCutMix**. The “Tagging” column indicates the source of memorization labels: “-” means no filtering was applied.

| Tagging | Methods | Mem. Ratio (%) ↓ | Improv. | MLE (%) † | α -Precision (%) † | β -Recall (%) † | Shape Score (%) † | Trend Score (%) † | C2STV (%) † | DCR (%) | |
|----------|---------|------------------|--------------|-----------|---------------------------|-----------------------|-------------------|-------------------|--------------|--------------|--------------|
| Default | - | CTGAN | 12.83 ± 0.63 | - | 68.68 ± 0.21 | 68.95 ± 1.70 | 16.49 ± 0.55 | 85.04 ± 0.93 | 77.05 ± 2.47 | 61.89 ± 4.89 | 49.45 ± 0.80 |
| | CTGAN | CTGAN+DCM | 12.47 ± 0.07 | 2.81% ↓ | 72.37 ± 0.39 | 71.72 ± 0.74 | 16.64 ± 0.20 | 85.78 ± 0.70 | 76.85 ± 1.62 | 57.98 ± 3.09 | 48.48 ± 0.24 |
| | TabDDPM | CTGAN+DCM | 12.69 ± 0.32 | 1.09% ↓ | 71.41 ± 0.89 | 68.93 ± 0.94 | 16.09 ± 0.59 | 84.42 ± 1.03 | 75.38 ± 1.54 | 56.85 ± 4.31 | 50.49 ± 1.12 |
| | - | TVAE | 17.22 ± 0.43 | - | 72.24 ± 0.36 | 82.97 ± 0.37 | 20.57 ± 0.42 | 89.37 ± 0.54 | 83.36 ± 0.99 | 52.63 ± 0.37 | 51.33 ± 0.96 |
| | TVAE | TVAE+DCM | 16.32 ± 0.21 | 5.23% ↓ | 76.27 ± 0.25 | 85.49 ± 0.41 | 21.66 ± 0.19 | 90.36 ± 0.25 | 86.76 ± 5.13 | 54.81 ± 0.79 | 51.07 ± 1.35 |
| Shoppers | TabDDPM | TVAE+DCM | 16.54 ± 0.27 | 3.95% ↓ | 73.82 ± 0.40 | 80.89 ± 1.12 | 21.47 ± 1.28 | 89.58 ± 0.19 | 78.24 ± 1.28 | 53.27 ± 4.92 | 50.92 ± 2.49 |
| | - | CTGAN | 19.80 ± 1.15 | - | 83.22 ± 1.30 | 85.26 ± 5.17 | 26.67 ± 1.66 | 77.73 ± 0.50 | 86.48 ± 0.69 | 67.18 ± 5.84 | 48.54 ± 0.74 |
| | CTGAN | CTGAN+DCM | 18.71 ± 0.56 | 5.51% ↓ | 85.51 ± 0.46 | 83.51 ± 1.60 | 26.19 ± 0.82 | 78.23 ± 0.30 | 86.36 ± 0.47 | 68.85 ± 2.45 | 50.64 ± 1.11 |
| | TabDDPM | CTGAN+DCM | 18.58 ± 0.43 | 6.16% ↓ | 83.52 ± 0.53 | 80.21 ± 2.75 | 25.70 ± 1.22 | 77.49 ± 1.24 | 86.40 ± 0.62 | 66.03 ± 7.67 | 50.47 ± 2.27 |
| | - | TVAE | 23.17 ± 0.77 | - | 86.65 ± 0.48 | 50.32 ± 2.98 | 11.16 ± 1.33 | 74.75 ± 0.92 | 77.56 ± 1.11 | 21.29 ± 3.28 | 43.31 ± 0.65 |
| Adult | TVAE | TVAE+DCM | 20.30 ± 1.33 | 12.39% ↓ | 88.32 ± 0.29 | 51.12 ± 2.46 | 11.98 ± 0.58 | 75.02 ± 0.97 | 79.02 ± 0.12 | 22.99 ± 2.12 | 49.98 ± 2.55 |
| | TabDDPM | TVAE+DCM | 19.54 ± 0.95 | 14.76% ↓ | 88.43 ± 0.17 | 50.43 ± 3.45 | 12.08 ± 2.01 | 74.82 ± 0.25 | 78.37 ± 1.18 | 22.57 ± 3.68 | 47.26 ± 1.81 |
| | - | CTGAN | 21.68 ± 0.62 | - | 88.64 ± 0.32 | 78.15 ± 3.66 | 26.27 ± 0.67 | 82.43 ± 0.90 | 82.83 ± 0.93 | 63.64 ± 2.74 | 49.14 ± 0.27 |
| | CTGAN | CTGAN+DCM | 16.53 ± 0.88 | 23.75% ↓ | 88.45 ± 0.29 | 79.31 ± 1.04 | 23.31 ± 1.42 | 82.23 ± 0.23 | 82.80 ± 2.27 | 63.46 ± 3.43 | 48.13 ± 0.33 |
| | TabDDPM | CTGAN+DCM | 19.71 ± 0.32 | 9.09% ↓ | 87.87 ± 0.37 | 72.40 ± 4.17 | 25.56 ± 1.45 | 81.42 ± 1.91 | 81.15 ± 1.23 | 58.84 ± 2.46 | 50.00 ± 0.19 |
| Adult | - | TVAE | 30.78 ± 0.41 | - | 88.61 ± 0.49 | 92.34 ± 2.19 | 29.90 ± 1.00 | 82.71 ± 0.45 | 79.06 ± 0.90 | 48.67 ± 2.70 | 48.76 ± 0.25 |
| | TVAE | TVAE+DCM | 26.11 ± 0.45 | 15.17% ↓ | 88.12 ± 0.32 | 87.54 ± 1.24 | 31.54 ± 0.38 | 83.45 ± 0.84 | 78.57 ± 0.68 | 54.85 ± 5.05 | 48.81 ± 2.10 |
| | TabDDPM | TVAE+DCM | 28.68 ± 0.21 | 6.82% ↓ | 89.23 ± 0.38 | 85.50 ± 4.09 | 30.23 ± 3.81 | 82.36 ± 1.96 | 78.80 ± 2.50 | 54.48 ± 8.01 | 49.57 ± 0.35 |

6.4 Cross-Model Transferability of Memorization Signals

Table 4 evaluates whether memorization-prone samples identified by TabDDPM generalize to other models. We compare standard DCM, which uses model-specific memorization signals (e.g., CTGAN+DCM), against **DCM-TabDDPM**, which uses labels derived from TabDDPM’s training and applies them to CTGAN and TVAE.

Obs.1: We find that TabDDPM-derived labels are transferable. For instance, CTGAN+DCM reduces memorization by 23.75% on ADULT, while CTGAN+DCM-TabDDPM still achieves a 9.09% reduction. Similar trends are observed for TVAE across datasets. Although slightly less effective than model-specific labels, DCM-TabDDPM still yields clear gains.

Table 5: The real and generative samples by TadDDPM and TadDDPM with DCM in Adult dataset. DCM represents DynamicCutMix.

| Samples | Age | Workclass | fnlwgt | Education | Education.num | Marital Status | Occupation | Relationship | Race | Sex | Capital Gain | Capital Loss | Hours per Week | Native Country | Income |
|-------------|-------|-----------|-----------|-----------|---------------|----------------|------------|---------------|-------|--------|--------------|--------------|----------------|----------------|--------|
| Real | 42.0 | Private | 108362.0 | HS-grad | 9.0 | Divorced | Sales | Not-in-family | White | Female | 0.0 | 0.0 | 42.0 | United-States | <=50K |
| TadDDPM | 55.0 | Private | 107841.53 | HS-grad | 9.0 | Divorced | Sales | Not-in-family | White | Female | 0.0 | 0.0 | 68.07 | United-States | <=50K |
| TadDDPM+DCM | 38.0 | Private | 110753.5 | HS-grad | 9.0 | Divorced | Sales | Not-in-family | Black | Female | 0.0 | 0.0 | 40.0 | United-States | <=50K |
| Real | 21.0 | Private | 185251.0 | HS-grad | 9.0 | Never-married | Sales | Own-child | White | Male | 0.0 | 0.0 | 40.0 | United-States | <=50K |
| TadDDPM | 24.54 | Private | 185105.25 | HS-grad | 9.0 | Never-married | Sales | Own-child | White | Male | 0.0 | 0.0 | 24.78 | United-States | <=50K |
| TadDDPM+DCM | 18.0 | Private | 187309.42 | HS-grad | 9.0 | Never-married | Sales | Own-child | White | Male | 0.0 | 0.0 | 25.0 | United-States | <=50K |

Obs.2: DCM-TabDDPM maintains model utility. Core metrics such as Shape Score and Trend Score remain stable, with minor trade-offs in some cases. For example, TVAE+DCM-TabDDPM reaches a shape score of 89.58% on DEFAULT, close to the 90.36% of model-specific DCM.

These results suggest that memorization signals from TabDDPM are robust and broadly useful, making DCM applicable even in settings without access to full training traces from the target model. Additional experimental results are provided in Appendix A.4.

6.5 Case Study on Adult Dataset: Real vs. Generated Samples

Table 5 presents representative examples from the Adult dataset comparing real samples, TadDDPM-generated samples, and those generated with DCM.

Obs.1: TadDDPM often generates samples closely resembling real data, with categorical features largely unchanged and only slight variations in numeric fields, indicating memorization.

Obs.2: DCM introduces greater variation in continuous attributes like age and working hours while preserving coherence in categorical features. For instance, the memorization ratio rises from 0.0971 to 0.7598, indicating the sample is no longer memorized.

7 Conclusions

We study memorization dynamics in tabular diffusion models from a data-centric perspective and find that a small subset of samples is memorized early and disproportionately. Leveraging this, we propose DynamicCut to filter high-risk samples using early memorization signals, and DynamicCutMix to combine filtering with feature-level augmentation. Our methods are simple, model-agnostic, and effective across datasets and architectures, reducing memorization while preserving data quality

and generalizing across generative models. Limitations and future directions are discussed in Appendix B.1 and B.2.

References

- Patricia A. Apellániz, Juan Parras, and Santiago Zazo. An improved tabular data generator with vae-gmm integration, 2024. URL <https://arxiv.org/abs/2404.08434>.
- Samuel A Assefa, Danial Dervovic, Mahmoud Mahfouz, Robert E Tillman, Prashant Reddy, and Manuela Veloso. Generating synthetic data in finance: opportunities, challenges and pitfalls. In *Proceedings of the First ACM International Conference on AI in Finance*, pages 1–8, 2020.
- Stella Biderman, Usvsn Prashanth, Lintang Sutawika, Hailey Schoelkopf, Quentin Anthony, Shivanshu Purohit, and Edward Raff. Emergent and predictable memorization in large language models. *Advances in Neural Information Processing Systems*, 36, 2024.
- Vadim Borisov, Kathrin Sessler, Tobias Leemann, Martin Pawelczyk, and Gjergji Kasneci. Language models are realistic tabular data generators. In *The Eleventh International Conference on Learning Representations*, 2023.
- Nicholas Carlini, Florian Tramer, Eric Wallace, Matthew Jagielski, Ariel Herbert-Voss, Katherine Lee, Adam Roberts, Tom Brown, Dawn Song, Ulfar Erlingsson, et al. Extracting training data from large language models. In *30th USENIX Security Symposium (USENIX Security 21)*, pages 2633–2650, 2021.
- Nitesh V Chawla, Kevin W Bowyer, Lawrence O Hall, and W Philip Kegelmeyer. Smote: synthetic minority over-sampling technique. *Journal of artificial intelligence research*, 16:321–357, 2002.
- Chen Chen, Daochang Liu, and Chang Xu. Towards memorization-free diffusion models. In *Proceedings of the IEEE/CVF Conference on Computer Vision and Pattern Recognition*, pages 8425–8434, 2024.
- Zhengyu Fang, Zhimeng Jiang, Huiyuan Chen, Xiao Li, and Jing Li. Understanding and mitigating memorization in diffusion models for tabular data. *arXiv preprint arXiv:2412.11044*, 2024.
- Joao Fonseca and Fernando Bacao. Tabular and latent space synthetic data generation: a literature review. *Journal of Big Data*, 10(1):115, 2023.
- Ian Goodfellow, Jean Pouget-Abadie, Mehdi Mirza, Bing Xu, David Warde-Farley, Sherjil Ozair, Aaron Courville, and Yoshua Bengio. Generative adversarial networks. *Communications of the ACM*, 63(11):139–144, 2020.
- Xiangming Gu, Chao Du, Tianyu Pang, Chongxuan Li, Min Lin, and Ye Wang. On memorization in diffusion models. *arXiv preprint arXiv:2310.02664*, 2023.
- Abhimanyu Hans, Yuxin Wen, Neel Jain, John Kirchenbauer, Hamid Kazemi, Prajwal Singhanian, Siddharth Singh, Gowthami Somepalli, Jonas Geiping, Abhinav Bhatele, et al. Be like a goldfish, don’t memorize! mitigating memorization in generative llms. *arXiv preprint arXiv:2406.10209*, 2024.
- Mikel Hernandez, Gorka Epelde, Ane Alberdi, Rodrigo Cilla, and Debbie Rankin. Synthetic data generation for tabular health records: A systematic review. *Neurocomputing*, 493:28–45, 2022.
- Dominik Hintersdorf, Lukas Struppek, Kristian Kersting, Adam Dziedzic, and Franziska Boenisch. Finding nemo: Localizing neurons responsible for memorization in diffusion models. *Advances in Neural Information Processing Systems*, 37:88236–88278, 2024.
- Jonathan Ho, Ajay Jain, and Pieter Abbeel. Denoising diffusion probabilistic models. *Advances in neural information processing systems*, 33:6840–6851, 2020.
- Jing Huang, Diyi Yang, and Christopher Potts. Demystifying verbatim memorization in large language models. *arXiv preprint arXiv:2407.17817*, 2024.

- Tero Karras, Miika Aittala, Timo Aila, and Samuli Laine. Elucidating the design space of diffusion-based generative models. *Advances in neural information processing systems*, 35:26565–26577, 2022.
- Jayoung Kim, Chaejeong Lee, and Noseong Park. Stasy: Score-based tabular data synthesis. In *The Eleventh International Conference on Learning Representations*, 2023.
- Diederik P Kingma. Auto-encoding variational bayes. *arXiv preprint arXiv:1312.6114*, 2013.
- Akim Kotelnikov, Dmitry Baranchuk, Ivan Rubachev, and Artem Babenko. Tabddpm: Modelling tabular data with diffusion models. *Proceedings of the 40th International Conference on Machine Learning (ICML)*, 202:17564–17579, 2023.
- Nupur Kumari, Bingliang Zhang, Sheng-Yu Wang, Eli Shechtman, Richard Zhang, and Jun-Yan Zhu. Ablating concepts in text-to-image diffusion models. In *Proceedings of the IEEE/CVF International Conference on Computer Vision*, pages 22691–22702, 2023.
- Chaejeong Lee, Jayoung Kim, and Noseong Park. Codi: Co-evolving contrastive diffusion models for mixed-type tabular synthesis. In *International Conference on Machine Learning*, pages 18940–18956. PMLR, 2023.
- Tennison Liu, Zhaozhi Qian, Jeroen Berrevoets, and Mihaela van der Schaar. Goggle: Generative modelling for tabular data by learning relational structure. In *The Eleventh International Conference on Learning Representations*, 2023.
- Junwei Ma, Apoorv Dankar, George Stein, Guangwei Yu, and Anthony Caterini. Tabpfn – tabular data generation with tabpfn, 2024. URL <https://arxiv.org/abs/2406.05216>.
- Noseong Park, Mahmoud Mohammadi, Kshitij Gorde, Sushil Jajodia, Hongkyu Park, and Youngmin Kim. Data synthesis based on generative adversarial networks. *Proceedings of the VLDB Endowment*, 11(10):1071–1083, June 2018. ISSN 2150-8097. doi: 10.14778/3231751.3231757. URL <http://dx.doi.org/10.14778/3231751.3231757>.
- Robin Rombach, Andreas Blattmann, Dominik Lorenz, Patrick Esser, and Björn Ommer. High-resolution image synthesis with latent diffusion models. In *Proceedings of the IEEE/CVF conference on computer vision and pattern recognition*, pages 10684–10695, 2022.
- Kulin Shah, Alkis Kalavasis, Adam R Klivans, and Giannis Daras. Does generation require memorization? creative diffusion models using ambient diffusion. *arXiv preprint arXiv:2502.21278*, 2025.
- Juntong Shi, Minkai Xu, Harper Hua, Hengrui Zhang, Stefano Ermon, and Jure Leskovec. Tabdiff: a mixed-type diffusion model for tabular data generation, 2025. URL <https://arxiv.org/abs/2410.20626>.
- Gowthami Somepalli, Vasu Singla, Micah Goldblum, Jonas Geiping, and Tom Goldstein. Diffusion art or digital forgery? investigating data replication in diffusion models. In *Proceedings of the IEEE/CVF Conference on Computer Vision and Pattern Recognition*, pages 6048–6058, 2023a.
- Gowthami Somepalli, Vasu Singla, Micah Goldblum, Jonas Geiping, and Tom Goldstein. Understanding and mitigating copying in diffusion models. *Advances in Neural Information Processing Systems*, 36:47783–47803, 2023b.
- Yang Song, Jascha Sohl-Dickstein, Diederik P Kingma, Abhishek Kumar, Stefano Ermon, and Ben Poole. Score-based generative modeling through stochastic differential equations. In *International Conference on Learning Representations*, 2021.
- Gerrit van den Burg and Chris Williams. On memorization in probabilistic deep generative models. *Advances in neural information processing systems*, 34:27916–27928, 2021.
- Yuxin Wen, Yuchen Liu, Chen Chen, and Lingjuan Lyu. Detecting, explaining, and mitigating memorization in diffusion models. In *The Twelfth International Conference on Learning Representations*, 2024.

- Lei Xu, Maria Skoularidou, Alfredo Cuesta-Infante, and Kalyan Veeramachaneni. Modeling tabular data using conditional gan. *Advances in neural information processing systems*, 32, 2019.
- Zeyu Yang, Peikun Guo, Khadija Zanna, and Akane Sano. Balanced mixed-type tabular data synthesis with diffusion models. *arXiv preprint arXiv:2404.08254*, 2024.
- TaeHo Yoon, Joo Young Choi, Sehyun Kwon, and Ernest K Ryu. Diffusion probabilistic models generalize when they fail to memorize. In *ICML 2023 Workshop on Structured Probabilistic Inference & Generative Modeling*, 2023.
- Hengrui Zhang, Jiani Zhang, Balasubramaniam Srinivasan, Zhengyuan Shen, Xiao Qin, Christos Faloutsos, Huzefa Rangwala, and George Karypis. Mixed-type tabular data synthesis with score-based diffusion in latent space. *arXiv preprint arXiv:2310.09656*, 2023.
- Yishuo Zhang, Nayyar A. Zaidi, Jiahui Zhou, and Gang Li. Ganblr: A tabular data generation model. In *2021 IEEE International Conference on Data Mining (ICDM)*, pages 181–190, 2021. doi: 10.1109/ICDM51629.2021.00103.

A More Experimental Results

A.1 Experiments on More Tag Ratios

A.1.1 Overall Performance Comparison

To understand how the tag ratio p used to identify high-memorization samples affects DynamicCut’s effectiveness, we conduct experiments across three different tag ratios: $p = 5\%$, 10% , and 20% on the SHOPPERS and ADULT datasets, as shown in Table 6. We have the following observations:

Obs. 1: On both SHOPPERS and ADULT, setting $p = 10\%$ consistently yields the most substantial memorization reduction—22.73% and 15.29%, respectively—outperforming both smaller ($p = 5\%$) and larger ($p = 20\%$) ratios. This indicates that a moderate filtering threshold balances aggressiveness and reliability in identifying memorization-prone samples.

Obs. 2: While the $p = 5\%$ setting is more conservative, the memorization reduction is weakest, and in some cases, utility metrics (e.g., β -Recall) degrade more than with $p = 10\%$. Conversely, using $p = 20\%$ introduces less precise filtering, leading to less effective memorization mitigation and inconsistent gains across utility metrics.

These results suggest that using a 10% threshold for filtering strikes the best trade-off between memorization suppression and generation quality, and we adopt $p = 10\%$ as the default setting for DynamicCut.

Table 6: Ablation study on the ratio p used for selecting high-memorization samples to filter in DynamicCut. “DCM 5%”, “DCM 10%”, and “DCM 20%” refer to retaining only the top- p fraction of memorized samples (according to warm-up Mem-AUC) for filtering. “Improv.” reports the relative memorization reduction compared to base TabDDPM. Results are shown for SHOPPERS and ADULT.

| | Methods | Mem. Ratio (%) ↓ | Improv. | MLE (%) ↑ | α -Precision (%) ↑ | β -Recall (%) ↑ | Shape Score (%) ↑ | Trend Score (%) ↑ | C2ST (%) ↑ | DCR (%) |
|----------|-----------------|------------------|----------|--------------|---------------------------|-----------------------|-------------------|-------------------|--------------|--------------|
| Shoppers | TabDDPM | 31.37 ± 0.31 | - | 92.17 ± 0.32 | 93.16 ± 1.58 | 52.57 ± 1.30 | 97.08 ± 0.46 | 92.92 ± 3.27 | 86.74 ± 0.63 | 51.36 ± 0.63 |
| | TabDDPM+DCM 5% | 28.43 ± 1.76 | 9.37% ↓ | 93.30 ± 0.22 | 94.49 ± 1.87 | 49.07 ± 2.35 | 95.98 ± 1.14 | 92.04 ± 1.81 | 84.66 ± 3.35 | 51.28 ± 1.28 |
| | TabDDPM+DCM 10% | 24.24 ± 2.83 | 22.73% ↓ | 91.46 ± 0.74 | 93.25 ± 3.87 | 46.15 ± 4.42 | 92.32 ± 5.00 | 89.11 ± 4.95 | 80.56 ± 4.81 | 49.74 ± 3.34 |
| | TabDDPM+DCM 20% | 29.40 ± 0.40 | 6.28% ↓ | 91.58 ± 0.51 | 91.66 ± 2.77 | 52.98 ± 1.99 | 95.30 ± 1.88 | 91.83 ± 1.35 | 82.69 ± 4.29 | 52.44 ± 0.33 |
| | TabDDPM | 31.01 ± 0.18 | - | 91.09 ± 0.07 | 93.58 ± 1.99 | 51.52 ± 2.29 | 98.84 ± 0.03 | 97.78 ± 0.07 | 94.63 ± 1.19 | 51.56 ± 0.34 |
| Adult | TabDDPM+DCM 5% | 27.63 ± 1.41 | 10.90% ↓ | 90.91 ± 0.26 | 95.73 ± 2.92 | 45.56 ± 2.63 | 98.08 ± 0.48 | 96.14 ± 1.50 | 90.21 ± 3.35 | 51.06 ± 0.56 |
| | TabDDPM+DCM 10% | 26.27 ± 0.57 | 15.29% ↓ | 90.81 ± 0.16 | 95.23 ± 1.14 | 45.76 ± 1.02 | 98.27 ± 0.32 | 96.71 ± 0.86 | 92.64 ± 1.65 | 50.79 ± 0.46 |
| | TabDDPM+DCM 20% | 26.09 ± 0.82 | 15.87% ↓ | 90.63 ± 0.31 | 94.75 ± 2.10 | 44.45 ± 0.83 | 98.03 ± 0.50 | 94.79 ± 1.88 | 91.01 ± 2.39 | 50.85 ± 0.24 |
| | TabDDPM | 31.01 ± 0.18 | - | 91.09 ± 0.07 | 93.58 ± 1.99 | 51.52 ± 2.29 | 98.84 ± 0.03 | 97.78 ± 0.07 | 94.63 ± 1.19 | 51.56 ± 0.34 |

A.1.2 Temporal Dynamics of Memorization

Figure 6 presents the cumulative proportion of memorized samples across training epochs for Top and Non-Top groups. Compared to the 5% results shown in the main paper, this figure includes additional curves for Top 10% and Top 20% samples, demonstrating that the early memorization trend persists across broader thresholds.

A.1.3 Temporal Dynamics of Forgetting

Figure 7 and Figure 8 extend the forgetting analysis in the main paper by including Top 10% and Top 20% groups in addition to the Top 5%. The results confirm that higher-memorization samples consistently exhibit earlier and more frequent forgetting behavior across all thresholds.

A.2 Experiments on More Datasets

To further assess the robustness and transferability of DCM, we conduct additional experiments on two diverse datasets, as shown in Table 7: CARDIO and WILT. These datasets differ significantly from the main benchmarks in size, structure, and difficulty, offering a more comprehensive evaluation of DCM’s generalizability. We compare TabDDPM enhanced with DCM against several strong augmentation baselines including SMOTE, TCM, and TCMP.

Obs.1: DCM maintains competitive or superior performance across both datasets. On CARDIO, although TCMP achieves the lowest memory ratio (23.05%), DCM maintains a comparably low memory usage (24.07%) while attaining the highest Shape Score (99.19%), a top-level Trend Score (98.72%), and the best DCR (50.93%). This reflects a strong balance between diversity and fidelity.

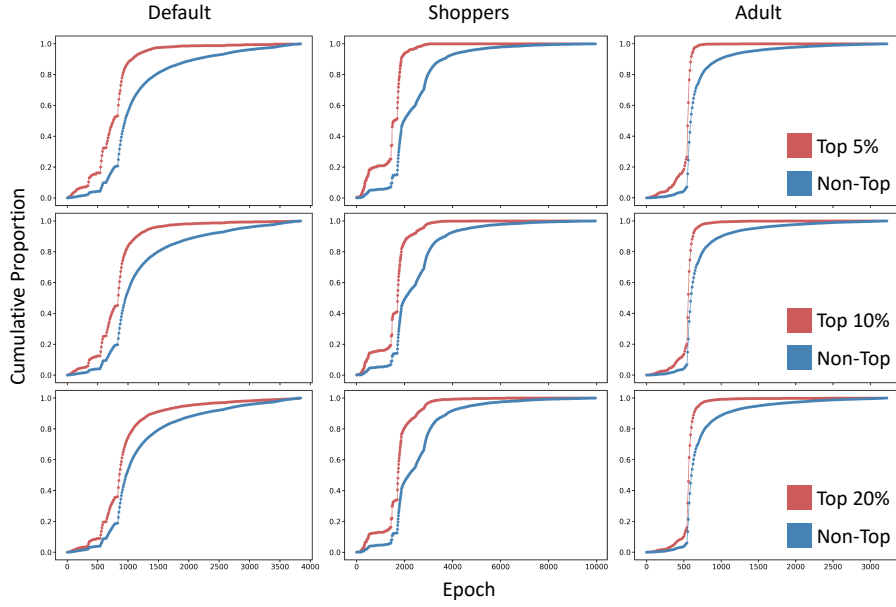


Figure 6: Cumulative proportion of samples memorized over epochs for Top and Non-Top groups.

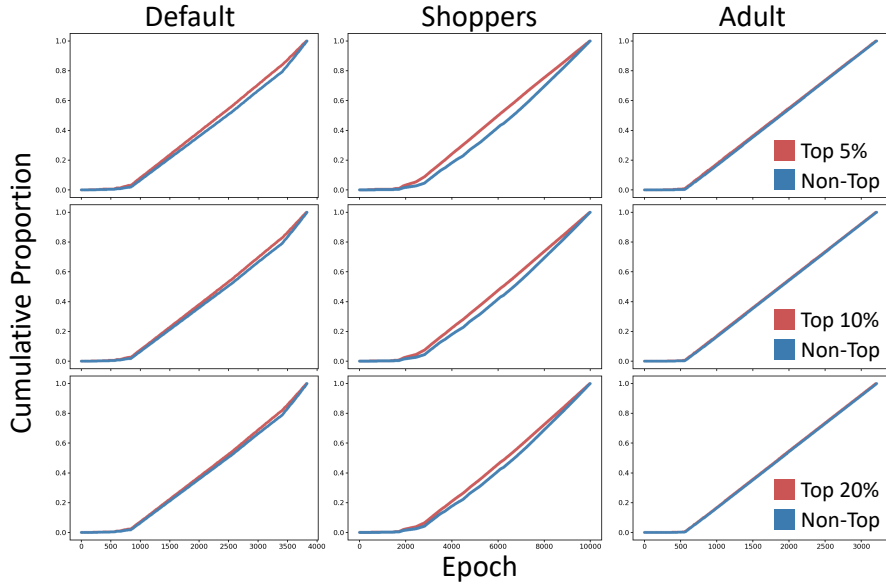


Figure 7: Dynamic changes in the number of forget events over training epochs for different groups.

On WILT, DCM outperforms all other methods in key distributional metrics. While reducing the memory ratio to 96.59%, DCM achieves the highest α -Precision (98.84%), a strong Trend Score (95.75%), and a superior DCR (51.08%), surpassing both TCMP and SMOTE. Notably, DCM avoids the significant performance degradation in β -Recall and C2ST observed with SMOTE, highlighting its ability to preserve minority modes without compromising sample quality.

These results provide further evidence that DCM generalizes beyond standard benchmarks and remains effective across a range of dataset characteristics.

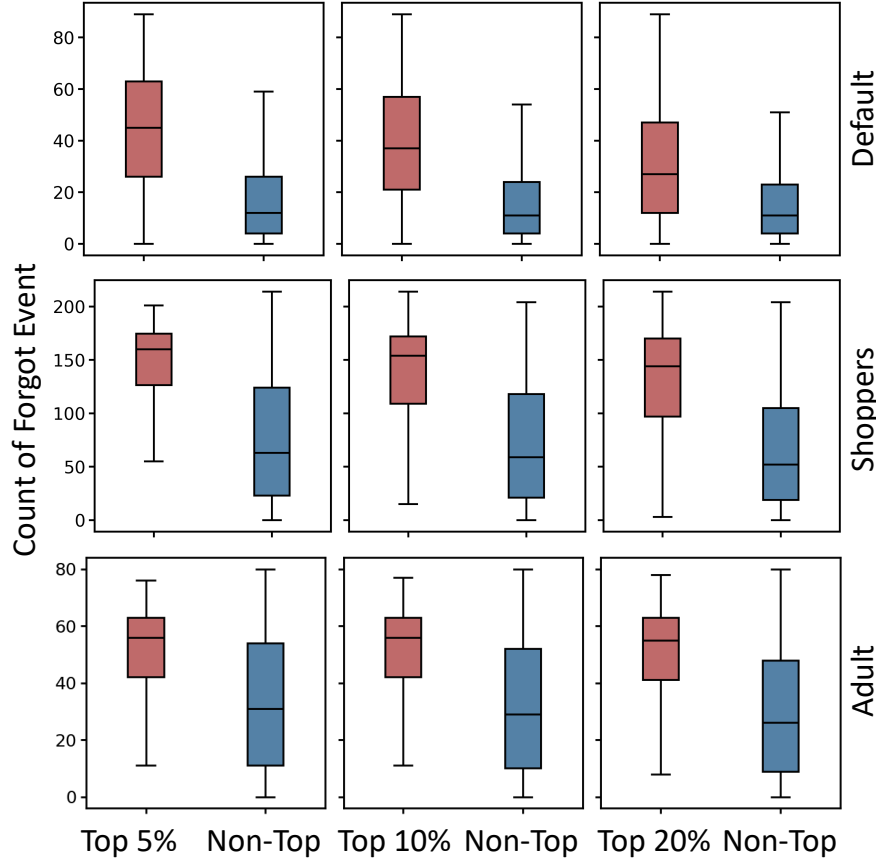


Figure 8: Dynamic changes in the number of forget events over training epochs for different groups.

Table 7: Additional evaluation of tabular generative models on supplementary datasets. “DCM” denotes our proposed **DynamicCutMix** method.

| | Methods | Mem. Ratio (%) ↓ | Improv. | MLE (%) ↑ | α -Precision (%) ↑ | β -Recall (%) ↑ | Shape Score (%) ↑ | Trend Score (%) ↑ | C2ST (%) ↑ | DCR (%) |
|--------|---------------|------------------|---------|--------------|---------------------------|-----------------------|-------------------|-------------------|--------------|--------------|
| Cardio | TabDDPM | 24.63 ± 0.18 | - | 80.24 ± 0.78 | 99.14 ± 0.15 | 49.11 ± 0.17 | 99.61 ± 0.03 | 98.95 ± 0.30 | 99.43 ± 0.55 | 49.91 ± 0.36 |
| | TabDDPM+SMOTE | 23.10 ± 0.69 | 6.21% ↓ | 79.47 ± 0.45 | 96.35 ± 2.38 | 47.44 ± 1.17 | 96.58 ± 0.75 | 94.39 ± 1.28 | 85.43 ± 1.69 | 50.73 ± 0.19 |
| | TabDDPM+TCM | 23.05 ± 0.38 | 6.40% ↓ | 79.71 ± 0.58 | 97.82 ± 2.05 | 48.37 ± 1.11 | 98.66 ± 1.35 | 95.86 ± 3.43 | 96.31 ± 0.42 | 49.24 ± 1.58 |
| | TabDDPM+TCMP | 23.54 ± 0.34 | 4.43% ↓ | 79.82 ± 0.27 | 98.71 ± 0.49 | 48.87 ± 0.34 | 98.88 ± 0.62 | 98.67 ± 0.20 | 96.31 ± 0.42 | 49.34 ± 0.38 |
| | TabDDPM+DCM | 24.07 ± 0.24 | 2.27% ↓ | 79.41 ± 0.46 | 98.92 ± 0.62 | 48.84 ± 0.14 | 99.19 ± 0.36 | 98.72 ± 0.32 | 97.38 ± 0.65 | 50.93 ± 0.40 |
| Wilt | TabDDPM | 98.48 ± 0.35 | - | 99.32 ± 0.58 | 98.63 ± 0.73 | 50.53 ± 0.47 | 98.58 ± 1.51 | 98.48 ± 0.35 | 98.63 ± 1.68 | 52.47 ± 0.54 |
| | TabDDPM+SMOTE | 96.78 ± 0.41 | 1.72% ↓ | 99.22 ± 0.54 | 79.49 ± 0.78 | 43.76 ± 1.37 | 91.09 ± 0.50 | 88.04 ± 4.73 | 76.66 ± 2.61 | 50.29 ± 0.28 |
| | TabDDPM+TCM | 97.17 ± 0.12 | 1.33% ↓ | 99.22 ± 0.38 | 97.93 ± 1.01 | 48.47 ± 1.17 | 97.31 ± 1.28 | 95.71 ± 2.49 | 96.92 ± 1.72 | 48.75 ± 2.18 |
| | TabDDPM+TCMP | 96.75 ± 0.67 | 1.76% ↓ | 99.52 ± 0.37 | 98.55 ± 0.14 | 49.36 ± 0.99 | 97.12 ± 0.84 | 96.81 ± 0.63 | 96.76 ± 3.44 | 45.52 ± 1.35 |
| | TabDDPM+DCM | 96.59 ± 0.32 | 1.92% ↓ | 98.49 ± 0.42 | 98.84 ± 0.25 | 47.00 ± 0.40 | 97.02 ± 0.88 | 95.75 ± 2.18 | 93.62 ± 0.67 | 51.08 ± 0.53 |

A.3 Hyperparameter Study on Pooling Strategy

We examined how different pooling strategies for warm-up Mem-AUC scores influence DynamicCut’s ability to spot high-memorization samples. Three variants were compared: (1) **Mean pooling** (DCM-Mean) – averages Mem-AUC across all warm-up epochs; (2) **Max pooling** (DCM-Max) – takes each sample’s single highest Mem-AUC., and (3) **top-10% mean pooling** (DCM-Top-Mean) – averages only the top-10% highest Mem-AUC epochs for each sample. As shown in Table 8, we have the following observations:

Obs. 1: Top-10% mean is consistently best for memorization mitigation. It delivers the largest memorization drop on both datasets, cutting memorization by 18.31% on Default and 22.73% on Shoppers relative to the TabDDPM baseline

Obs. 2: Max pooling trades memorization for marginal utility gains. DCM-Max occasionally posts slightly better utility metrics such as MLE, but its memorization reduction is smaller and less consistent.

Obs. 3: Mean pooling is balanced but never optimal. DCM-Mean offers moderate improvements across metrics yet fails to beat the top-10% strategy in either privacy or quality.

These results suggest that computing the memorization score based on the most salient epochs offers a more reliable signal for identifying high-risk samples. Therefore, we adopt **top-10% mean** as the default pooling method in our DynamicCut implementation.

Table 8: Comparison of different pooling strategies used to compute memorization scores for filtering. “DCM-Mean,” “DCM-Max,” and “DCM-Top-Mean” denote the use of mean, max, and top-10% mean pooling over the warm-up phase Mem-AUC sequence, respectively. “Improv.” indicates the relative memorization reduction over the base TabDDPM.

| Methods | Mem. Ratio (%) ↓ | Improv. | MLE (%) ↑ | α -Precision (%) ↑ | β -Recall (%) ↑ | Shape Score (%) ↑ | Trend Score (%) ↑ | C2ST (%) ↑ | DCR (%) |
|----------------------|------------------|----------|--------------|---------------------------|-----------------------|-------------------|-------------------|---------------|--------------|
| Default | | | | | | | | | |
| TabDDPM | 19.33 ± 0.45 | - | 76.79 ± 0.69 | 98.15 ± 1.45 | 44.41 ± 0.70 | 97.58 ± 0.95 | 94.46 ± 0.68 | 91.85 ± 6.04 | 49.12 ± 0.94 |
| TabDDPM+DCM-Mean | 17.12 ± 0.78 | 11.43% ↓ | 79.55 ± 0.70 | 95.92 ± 3.21 | 38.94 ± 0.98 | 96.21 ± 1.33 | 90.23 ± 0.88 | 87.35 ± 4.42 | 50.64 ± 0.94 |
| TabDDPM+DCM-Max | 16.67 ± 1.22 | 13.76% ↓ | 80.09 ± 0.55 | 91.08 ± 7.60 | 37.93 ± 3.26 | 94.59 ± 3.32 | 90.51 ± 3.52 | 88.47 ± 7.36 | 49.32 ± 2.63 |
| TabDDPM+DCM-Top-Mean | 15.79 ± 2.06 | 18.31% ↓ | 76.68 ± 0.76 | 91.97 ± 1.78 | 37.89 ± 0.84 | 93.62 ± 2.78 | 89.30 ± 3.02 | 87.63 ± 2.15 | 48.17 ± 2.59 |
| Shoppers | | | | | | | | | |
| TabDDPM | 31.37 ± 0.31 | - | 92.17 ± 0.32 | 93.16 ± 1.58 | 52.57 ± 1.30 | 97.08 ± 0.46 | 92.92 ± 3.27 | 86.74 ± 0.63 | 51.36 ± 0.63 |
| TabDDPM+DCM-Mean | 27.33 ± 1.12 | 12.88% ↓ | 92.58 ± 0.42 | 95.66 ± 0.61 | 48.54 ± 0.70 | 94.12 ± 2.01 | 91.47 ± 1.07 | 82.01 ± 2.73 | 51.00 ± 2.91 |
| TabDDPM+DCM-Max | 26.68 ± 2.75 | 14.95% ↓ | 93.21 ± 0.32 | 91.93 ± 6.24 | 47.97 ± 3.22 | 94.34 ± 4.12 | 90.50 ± 5.55 | 80.66 ± 11.39 | 49.59 ± 1.86 |
| TabDDPM+DCM-Top-Mean | 24.24 ± 2.83 | 22.73% ↓ | 91.46 ± 0.74 | 93.25 ± 3.87 | 46.15 ± 4.42 | 92.32 ± 5.00 | 89.11 ± 4.95 | 80.56 ± 4.81 | 49.74 ± 3.34 |

A.4 Experiments on Transferability

To further evaluate the transferability of memorization labels across generative models, we visualize memorization ratios under different labeling-training combinations for each dataset in Figure 9. For each heatmap, the row indicates the model used to generate memorization labels (e.g., TabDDPM), and the column indicates the model trained using those labels for DCM filtering.

Obs. 1: Across all three datasets (DEFAULT, SHOPPERS, ADULT), we observe that model-specific labels (diagonal entries) consistently achieve the lowest memorization ratios. This suggests that using labels generated by the same model provides the most precise filtering guidance during training.

Obs. 2: Notably, labels derived from TabDDPM generalize well to other architectures, achieving the second-best memorization reduction in most off-diagonal cases. For example, TabDDPM-generated labels significantly reduce memorization when applied to CTGAN and TVAE, outperforming those generated by weaker models such as TVAE.

These results confirm that memorization-prone samples identified by a strong base model (e.g., TabDDPM) can be effectively reused across other generative models for filtering, demonstrating the robustness and practical value of our transferability approach.

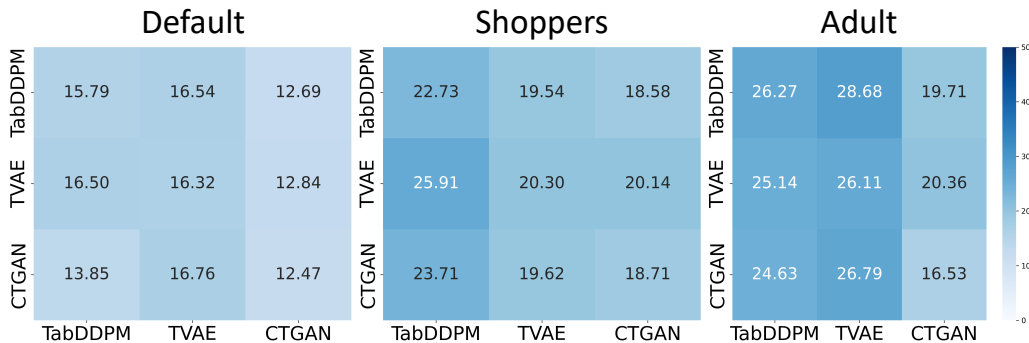


Figure 9: Heatmaps showing memorization ratios (%) for different label-source and model-target combinations on DEFAULT, SHOPPERS, and ADULT datasets. Rows denote the model used to generate memorization labels, and columns denote the model trained with those labels.

A.5 Experiments on Memorization Tag Performance

To assess the quality of memorization labels generated during the warm-up phase, we compute the average AUC of classifiers trained to predict whether a sample will exhibit high memorization frequency. As shown in Table 9, the AUC values range from 73.78% on DEFAULT to 80.14% on SHOPPERS, indicating a strong alignment between early-phase memorization behavior and the final memorization frequency observed during training.

Obs: These results suggest that warm-up memorization dynamics can serve as a reliable signal for identifying memorization-prone samples. The consistent AUC scores across datasets validate the effectiveness of our warm-up labeling strategy in capturing meaningful patterns relevant to memorization, and support its use as a filtering criterion in DynamicCut.

Table 9: AUC scores of memorization tag classifiers trained using warm-up phase labels across three datasets. Higher AUC indicates better agreement between early-phase tags and final high memorization frequency samples.

| Dataset | Average AUC |
|----------|-------------|
| Default | 73.78% |
| Shoppers | 80.14% |
| Adult | 76.52% |

A.6 Experiments on Data Generation Quality

A.6.1 Feature Correlation Matrix Comparison

To assess whether DCM affects the structural fidelity of synthetic data, we compare the absolute divergence between the pairwise feature correlation matrices of the real and synthetic data. As shown in Figure 10, lighter colors indicate smaller divergences, implying better preservation of inter-feature relationships.

Obs: Across all three datasets (ADULT, DEFAULT, and SHOPPERS), the heatmaps show that DCM-filtered models produce correlation structures that are visually comparable to, and in some cases slightly better than, those from the base TabDDPM. The differences are minor, indicating that the memorization filtering introduced by DCM does not significantly alter the statistical dependencies among features.

These results demonstrate that DynamicCut can effectively reduce memorization without compromising the core structural quality of the generated data.

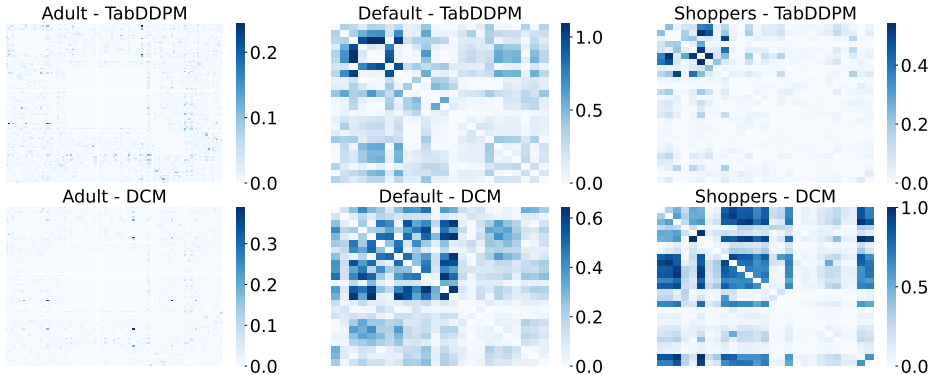


Figure 10: Heatmaps of the pair-wise column correlation of synthetic data v.s. the real data. The value represents the absolute divergence between the real and estimated correlations (the lighter, the better).

A.6.2 Shape Score

To further evaluate the quality of the synthetic data, we compare the shape score of each feature across datasets, as shown in Figure 11. The shape score measures the similarity between the marginal distributions of real and synthetic data, with higher values indicating better alignment.

Obs: Across all datasets—ADULT, DEFAULT, and SHOPPERS—the shape scores of TabDDPM and TabDDPM+DCM are closely matched for most features. In particular, for datasets like ADULT and DEFAULT, the scores remain above 0.95 in the majority of features, demonstrating that the marginal distributions are well-preserved even after memorization filtering. For SHOPPERS, although the feature variability is higher, DCM still maintains competitive shape scores relative to the base model.

These results confirm that DynamicCut achieves effective memorization reduction without degrading the fidelity of per-feature distributions, thus preserving a key aspect of data generation quality.

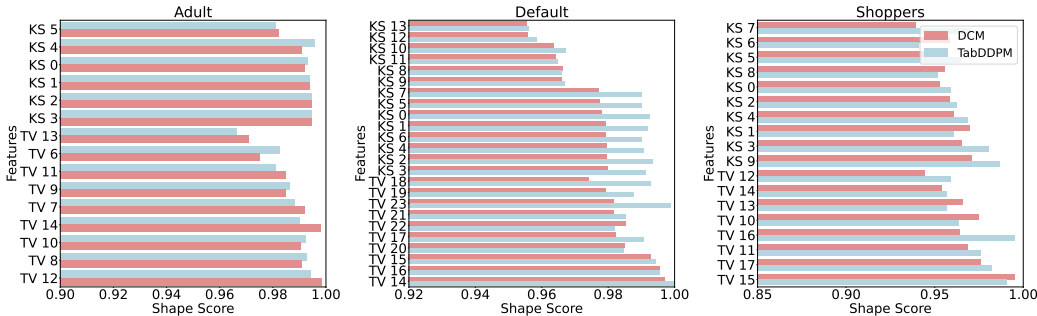


Figure 11: Shape score comparison for each feature in synthetic data generated by TabDDPM and TabDDPM+DCM across multiple datasets.

B Discussion

B.1 Limitation Discussion

While our work provides a principled and effective approach to reducing memorization in tabular diffusion models, it has several limitations.

First, our methods rely on tracking memorization signals during training, which requires generating and comparing synthetic samples at regular intervals. This may introduce additional computational overhead, especially for large-scale datasets or when extended to high-frequency monitoring.

Second, the effectiveness of DynamicCut depends on a warm-up phase that sufficiently exposes early memorization patterns. For models or datasets where such patterns emerge later, the current strategy may underperform or miss certain high-risk samples.

Third, the method introduces additional hyperparameters—such as the warm-up length, top- k selection ratio, and filtering percentage—which may affect performance. Although we use consistent settings across datasets, the optimal configuration may vary depending on data scale, feature types, and training dynamics.

We leave these directions for future exploration.

B.2 Future Work

Our study opens several promising directions for future research.

First, a deeper investigation into why certain samples are more prone to memorization is needed. In particular, exploring memorization at the feature level—such as which attributes contribute most to high memorization intensity—could improve interpretability and inform more targeted interventions.

Second, our current method uses a fixed warm-up phase to identify memorization-prone samples. Future work could explore adaptive or continuous memorization monitoring strategies that dynamically adjust to training progress or model uncertainty.

C Experimental Details

We implement DynamicCut and DynamicCutMix along with all baseline methods using the PyTorch framework. All models are trained using the Adam optimizer. Our code is available at <https://anonymous.4open.science/r/DynamicCut-8255>

C.1 Baselines of Data Augmentation

This section outlines the data augmentation methods evaluated in this work, including SMOTE, TabCutMix (TCM), and TabCutMixPlus (TCMP).

- **SMOTE**: The Synthetic Minority Oversampling Technique (SMOTE) Chawla et al. [2002] is a foundational oversampling method initially proposed to address class imbalance in datasets with continuous variables. It generates new minority class samples by interpolating feature values between existing samples and their k nearest neighbors. Although SMOTE is effective in enhancing diversity and reducing overfitting in fully numerical datasets, its design does not account for categorical attributes. Direct application to mixed-type data can therefore produce invalid or nonsensical feature combinations that violate feature semantics.
- **TabCutMix (TCM)**: TabCutMix (TCM) Fang et al. [2024] adapts the CutMix concept from computer vision to the tabular domain. TCM generates augmented samples by selectively replacing subsets of features between two instances from the same class, guided by a binary mask sampled from a Bernoulli distribution. The mask controls the replacement ratio λ , enabling partial feature replacement. By promoting intra-class variability while preserving label integrity, TCM improves generalization and reduces overfitting in mixed-type tabular learning tasks.
- **TabCutMixPlus (TCMP)**: TabCutMixPlus (TCMP) Fang et al. [2024] builds upon TCM by introducing dependency-aware feature augmentation. TCMP first performs feature clustering based on domain-relevant correlation metrics to identify groups of highly related features. Augmentation is then performed at the cluster level, ensuring that structurally or semantically related features are swapped together. This strategy helps maintain intra-cluster consistency, mitigates the risk of generating unrealistic data points, and enhances both diversity and robustness in the augmented dataset.

C.2 Baselines of Tabular Data Generation

This section describes the baseline generative models used in our study. These methods represent widely recognized approaches for synthesizing structured tabular data with mixed numerical and categorical attributes.

- **CTGAN** Xu et al. [2019]: CTGAN is a generative adversarial network (GAN) designed to address the unique challenges of tabular data generation. To better capture complex, skewed, or multimodal numerical feature distributions, CTGAN employs mode-specific normalization based on quantile transformation. Additionally, it leverages a conditional sampling strategy that focuses on rare categories when generating new samples. This conditional mechanism helps balance class distributions and promotes diversity across different feature values in the generated data.
- **TVAE** Xu et al. [2019]: TVAE extends the variational autoencoder (VAE) framework to handle tabular data. Like CTGAN, it applies mode-specific normalization and conditional generation techniques, but models data through a latent probabilistic structure by optimizing the Evidence Lower Bound (ELBO). This allows TVAE to learn a meaningful latent representation that captures dependencies between numerical and categorical features, facilitating the generation of realistic and diverse synthetic samples while maintaining scalability.
- **TabDDPM** Kotelnikov et al. [2023]: TabDDPM adapts denoising diffusion probabilistic models (DDPMs) for tabular data with mixed feature types. It applies continuous-time stochastic differential equations (SDEs) to latent representations of tabular samples, enabling score-based generative modeling. To jointly model numerical and categorical features, TabDDPM incorporates specialized feature embeddings and masking strategies within a unified diffusion framework. This design supports both unconditional and conditional sample generation, offering improved training stability and sample quality.

C.3 Quantifying Memorization

Generative models risk overfitting when they overly replicate samples from their training data instead of producing diverse, novel instances representative of the full underlying data distribution. While retaining some level of fidelity is beneficial in certain use cases—such as high-precision applications—over-memorization can hinder diversity, introduce privacy risks, and compromise the model’s ability to generalize. This issue is particularly relevant in tabular data scenarios, where direct reproduction of training records may lead to sensitive information leakage or limit the usefulness of generated data.

Relative Distance Ratio Criterion. To systematically evaluate the extent of memorization, we introduce the *relative distance ratio* as a sample-level diagnostic. Given a generated sample x and the training dataset \mathcal{D} , the distance ratio $r(x)$ is computed as:

$$r(x) = \frac{d(x, \text{NN}_1(x, \mathcal{D}))}{d(x, \text{NN}_2(x, \mathcal{D}))},$$

where $d(\cdot, \cdot)$ is a distance function in the data space, $\text{NN}_1(x, \mathcal{D})$ is the closest training sample to x , and $\text{NN}_2(x, \mathcal{D})$ is the second closest. A lower $r(x)$ indicates that x is unusually close to a single training point compared to others, signaling potential memorization.

Following best practices from the domain of image synthesis, we label a generated sample as *memorized* if its distance ratio falls below a threshold of $\frac{1}{3}$.

Memorization AUC. To capture how memorization varies over a range of sensitivity thresholds, we introduce the *Memorization Area Under the Curve (Mem-AUC)*. This metric aggregates the memorization ratio across all threshold values $\tau \in [0, 1]$, providing a comprehensive view of memorization intensity:

$$\text{Mem-AUC} = \int_0^1 \text{Mem. Ratio}(\tau) d\tau,$$

where $\text{Mem. Ratio}(\tau)$ denotes the fraction of generated samples with $r(x) < \tau$ for a given threshold τ .

Higher Mem-AUC values indicate stronger overall memorization tendencies, while lower values reflect better generalization and less replication of the training data. Together, the memorization ratio and Mem-AUC offer both fixed-threshold and threshold-sweeping perspectives on the memorization behavior of generative models.

Memorization Ratio. We define the *memorization ratio* as the fraction of generated samples that meet this memorization condition:

$$\text{Mem. Ratio} = \frac{1}{|\mathcal{G}|} \sum_{x \in \mathcal{G}} \mathbb{I}(r(x) < \frac{1}{3}),$$

where \mathcal{G} represents the set of generated instances and $\mathbb{I}(\cdot)$ is an indicator function. This score provides a single-point estimate of the prevalence of memorization in the generated dataset.

Tracking Memorization Dynamics. To move beyond a single, static memorization snapshot, we follow each real training sample *through epoch* and document when and how often it becomes memorized, forgotten, and re-memorized. Below we introduce the exact notation and event definitions that make this temporal analysis reproducible. We denote $\mathcal{D} = \{x_r\}_{r=1}^{|\mathcal{D}|}$ as training set, τ as a fixed memorization threshold (we adopt $\tau = \frac{1}{3}$), and $\mathcal{G}_e = \{x_{g,e}^{(j)}\}_{j=1}^{|\mathcal{G}_e|}$ as the samples generated *after* epoch $e \in \{1, \dots, E\}$.

For every real sample x_r and epoch e , we record a binary flag

$$\mathbb{1}_e(x_r) = \mathbb{I}\left[\exists x \in \mathcal{G}_e : r(x) < \tau \wedge \text{NN}_1(x, \mathcal{D}) = x_r\right],$$

where $\text{NN}_1(\cdot, \mathcal{D})$ returns the nearest neighbour in the training set. Intuitively, $\mathbb{1}_e(x_r) = 1$ means that, at epoch e , at least one generated sample sits “too close” to x_r , signalling potential leakage of that sample.

Event Definitions. We translate the per-epoch indicators into discrete events that mirror our informal reasoning about memorization behavior.

$$\text{FirstMem}(x_r) = \min\{e : \mathbb{1}_e(x_r) = 1\} \quad (\text{first epoch } x_r \text{ is memorized}),$$

$$\text{Forget}(x_r) = \{e : \mathbb{1}_{e-1}(x_r) = 1 \wedge \mathbb{1}_e(x_r) = 0\} \quad (\text{moments when } x_r \text{ stops being memorized}).$$

If $\text{FirstMem}(x_r)$ is undefined, the model never memorizes x_r .

Count Statistics. A single event seldom tells the full story. We therefore accumulate events into counts that capture temporal behaviors and volatility.

$$\text{CumMemCnt}(x_r) = \sum_{e=1}^E \mathbb{1}_e(x_r) \quad \text{total epochs during which } x_r \text{ is memorized,}$$

$$\text{CumForgetCnt}(x_r) = |\text{Forget}(x_r)| \quad \text{number of “un-memorization” transitions.}$$

High CumMemCnt indicates long-lasting leakage; a high CumForgetCnt suggests unstable or oscillatory behavior.

Instance-level Mem-AUC. To capture *how strongly* a sample x_r is memorized—independent of an arbitrary threshold—we integrate the conditional memorization probability over every possible threshold:

$$\text{Mem-AUC}(x_r) = \int_0^1 \Pr[r(x) < \tau \mid \text{NN}_1(x, \mathcal{D}) = x_r] d\tau.$$

Here, the probability is estimated over all $x \in \mathcal{G}_e$ and all epochs e . Larger values imply stronger, more persistent memorization. Such instance-level Mem-AUC provides a quantitative way to detect high-memorization samples based on temporal and memorization strength signal, such as top-10% (*high-risk*) and bottom-10% (*low-risk*) Mem-AUC subsets.

In a nutshell, these precise definitions underpin our analysis and pinpoint when memorization first emerges, how long it persists, and how often the model successfully “forgets” individual records. The temporal lens complements the static memorization ratio and provides a new dimension for memorization mitigation throughout training.

Table 10: Statistics of datasets. *Num* indicates the number of numerical columns, and *Cat* indicates the number of categorical columns.

| Dataset | #Rows | #Num | #Cat | #Train | #Validation | #Test | Task |
|----------|--------|------|------|--------|-------------|--------|----------------|
| Adult | 48,842 | 6 | 9 | 28,943 | 3,618 | 16,281 | Classification |
| Default | 30,000 | 14 | 11 | 24,000 | 3,000 | 3,000 | Classification |
| Shoppers | 12,330 | 10 | 8 | 9,864 | 1,233 | 1,233 | Classification |
| Cardio | 70,000 | 5 | 7 | 44,800 | 11,200 | 14,000 | Classification |
| Wilt | 4,839 | 5 | 1 | 3,096 | 775 | 968 | Classification |

C.4 Datasets

We conduct our experiments on three widely recognized benchmark datasets sourced from the UCI Machine Learning Repository. These datasets span diverse application domains, including income prediction, credit risk assessment, and online customer behavior analysis. Table 10 provides an overview of their key characteristics.

Detailed Dataset Summaries.

- **Adult Dataset**²: Also known as the Census Income dataset, this dataset contains demographic and employment information from the 1994 U.S. Census. The binary classification task aims to predict whether an individual’s annual income exceeds \$50,000. It consists of 48,842 records with features such as age, education, occupation, marital status, and work class. This dataset is commonly used in fairness, socio-economic, and income classification studies.

²<https://archive.ics.uci.edu/dataset/2/adult>

- **Default Dataset**³: This dataset includes 30,000 instances of credit card clients in Taiwan, featuring financial and demographic information collected between April and September 2005. The goal is to predict the likelihood of a client defaulting on their credit card payment in the next billing cycle. Key attributes include credit limit, payment history, bill amounts, and personal demographics, making it particularly relevant for financial risk modeling and credit scoring research.
- **Shoppers Dataset**⁴: Collected from user sessions on e-commerce platforms, this dataset consists of 12,330 records detailing user interaction patterns. Features include the number of pages visited, session durations, and various behavioral indicators. The binary target indicates whether a session ended with a purchase. This dataset serves as a benchmark for studying customer behavior, website optimization, and purchase intent prediction.
- **Wilt Dataset**⁵: This dataset originates from high-resolution remote sensing imagery and is designed for binary classification of vegetation health. The task involves distinguishing between healthy land cover (label 'n') and areas exhibiting signs of disease or stress (label 'w'), based on 4,889 observations. Each instance is described by spectral and textural attributes extracted from Quickbird satellite data, including metrics like GLCM mean texture, normalized color bands (green, red, NIR), and statistical features such as the standard deviation of the panchromatic band. The dataset is notably imbalanced, with only 74 samples labeled as diseased, presenting additional challenges for generative modeling and minority class preservation.
- **Cardio Dataset**⁶: This dataset contains anonymized health profiles of 70,000 individuals, collected for the purpose of predicting cardiovascular disease risk. The feature set spans 11 variables covering demographic information (e.g., age, gender, height, weight), clinical measurements (e.g., systolic and diastolic blood pressure, cholesterol levels, glucose concentration), and lifestyle indicators (e.g., smoking, alcohol use, physical activity). The binary target indicates whether a subject has been diagnosed with cardiovascular disease. The dataset is moderately imbalanced and has been widely used in evaluating tabular generative and classification models.

In Table 10, The column “# Rows” represents the number of records in each dataset, while “# Num” and “# Cat” indicate the number of numerical and categorical features (including the target feature), respectively. Each dataset is divided into training, validation, and testing sets for machine learning efficiency experiments. For the Adult dataset, which includes an official test set, we use this set directly for testing, and split the training set into training and validation sets with a ratio of 8 : 1. For the remaining datasets, the data is partitioned into training, validation, and test sets with a ratio of 8 : 1 : 1, ensuring consistent splitting using a fixed random seed.

³<https://archive.ics.uci.edu/dataset/350/default+of+credit+card+clients>

⁴<https://archive.ics.uci.edu/dataset/468/online+shoppers+purchasing+intention+dataset>

⁵<https://archive.ics.uci.edu/dataset/285/wilt>

⁶<https://www.kaggle.com/datasets/sulianova/cardiovascular-disease-dataset>